

# NIR Spectroscopy of Type Ia supernovae

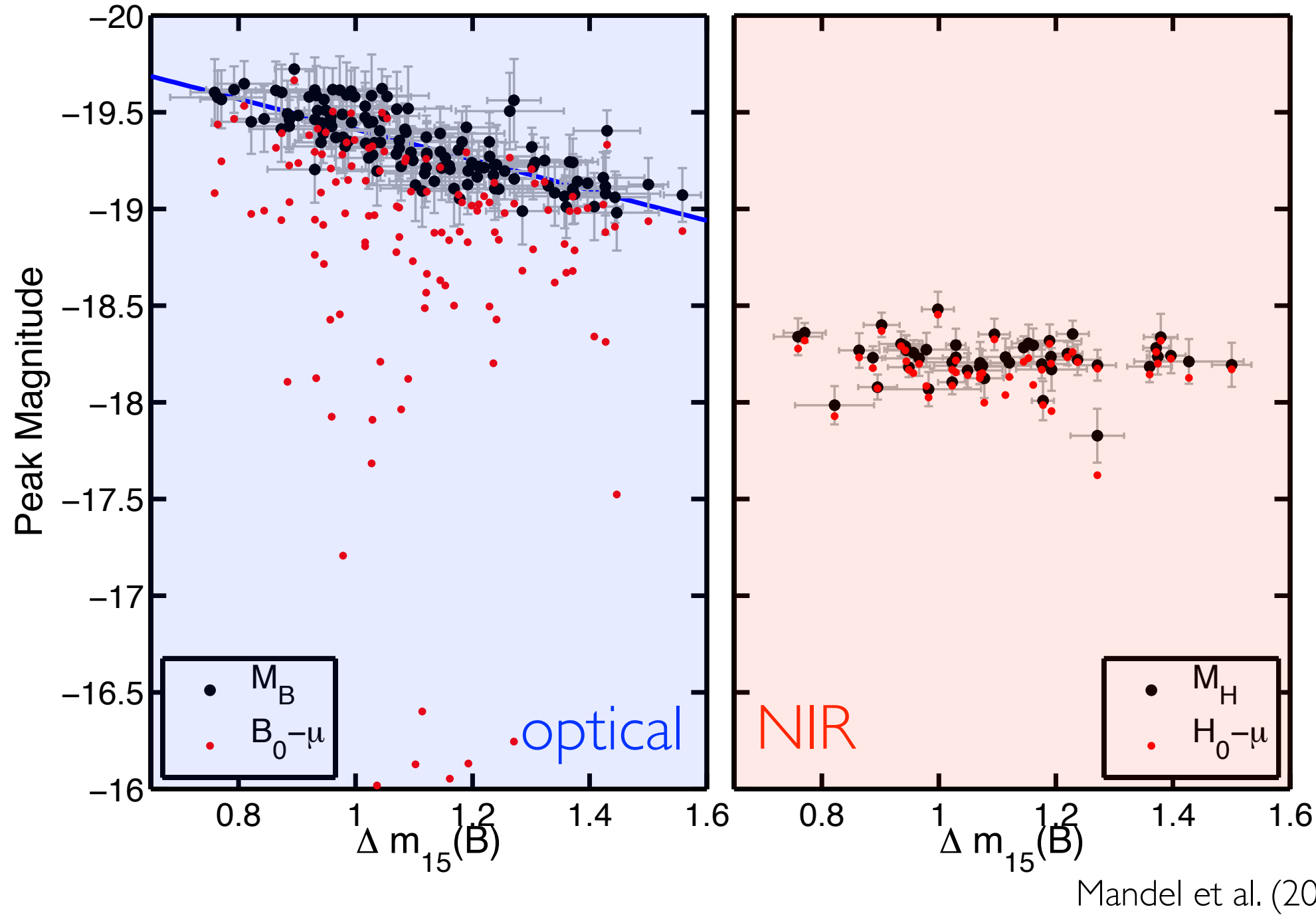
Mark Phillips,  
Chris Burns, Carlos Contreras,  
Tiara Diamond, Francisco Förster,  
Lluis Galbany, Peter Hoeflich,  
Mansi Kasliwal, Robert Kirshner,  
Howie Marion, Nidia Morrell,  
Dave Sand, Max Stritzinger,  
Lingzhi Wang, and many others.

Eric Y. Hsiao

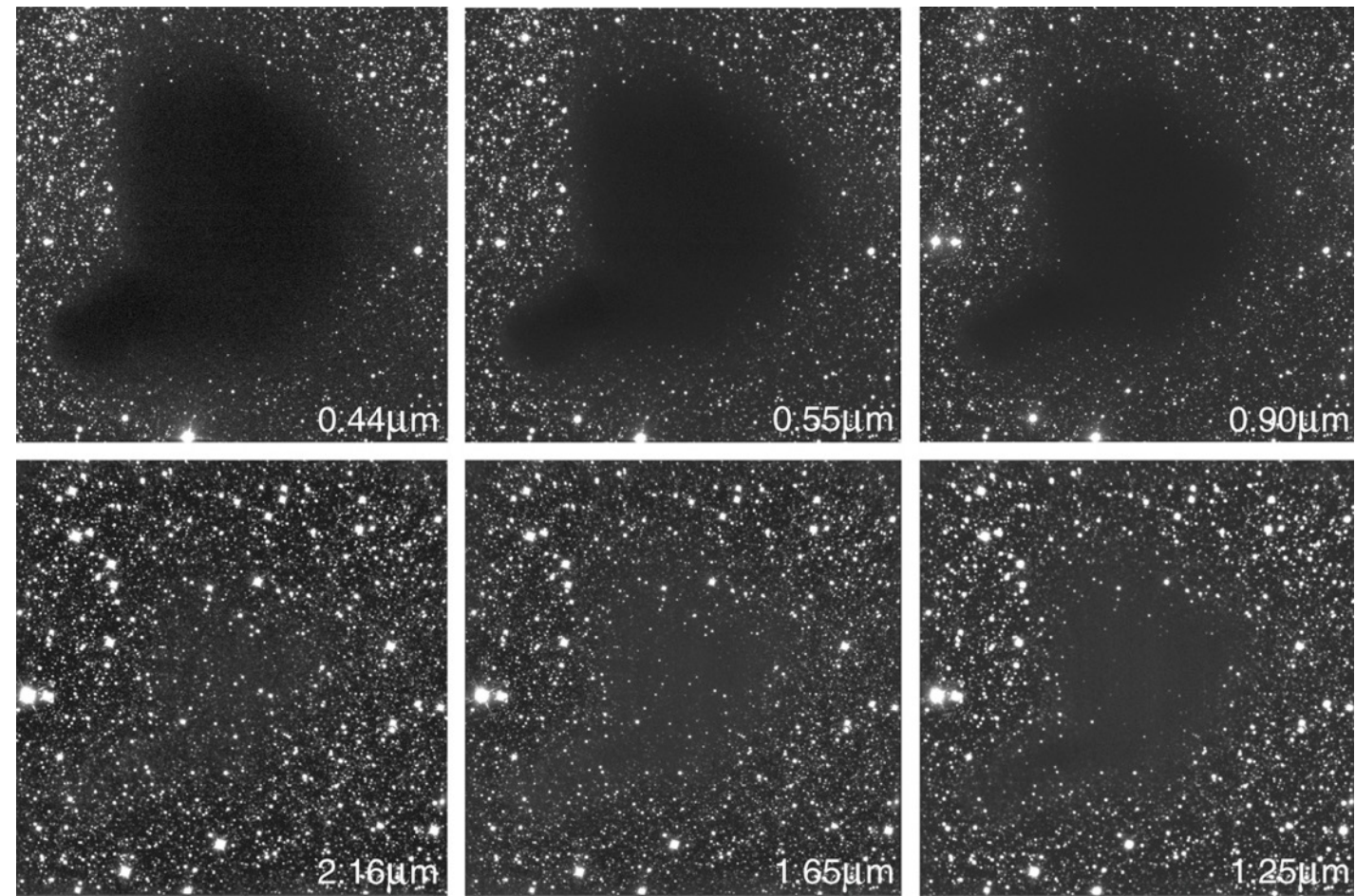
Florida State University



# Why NIR?



# Why NIR?

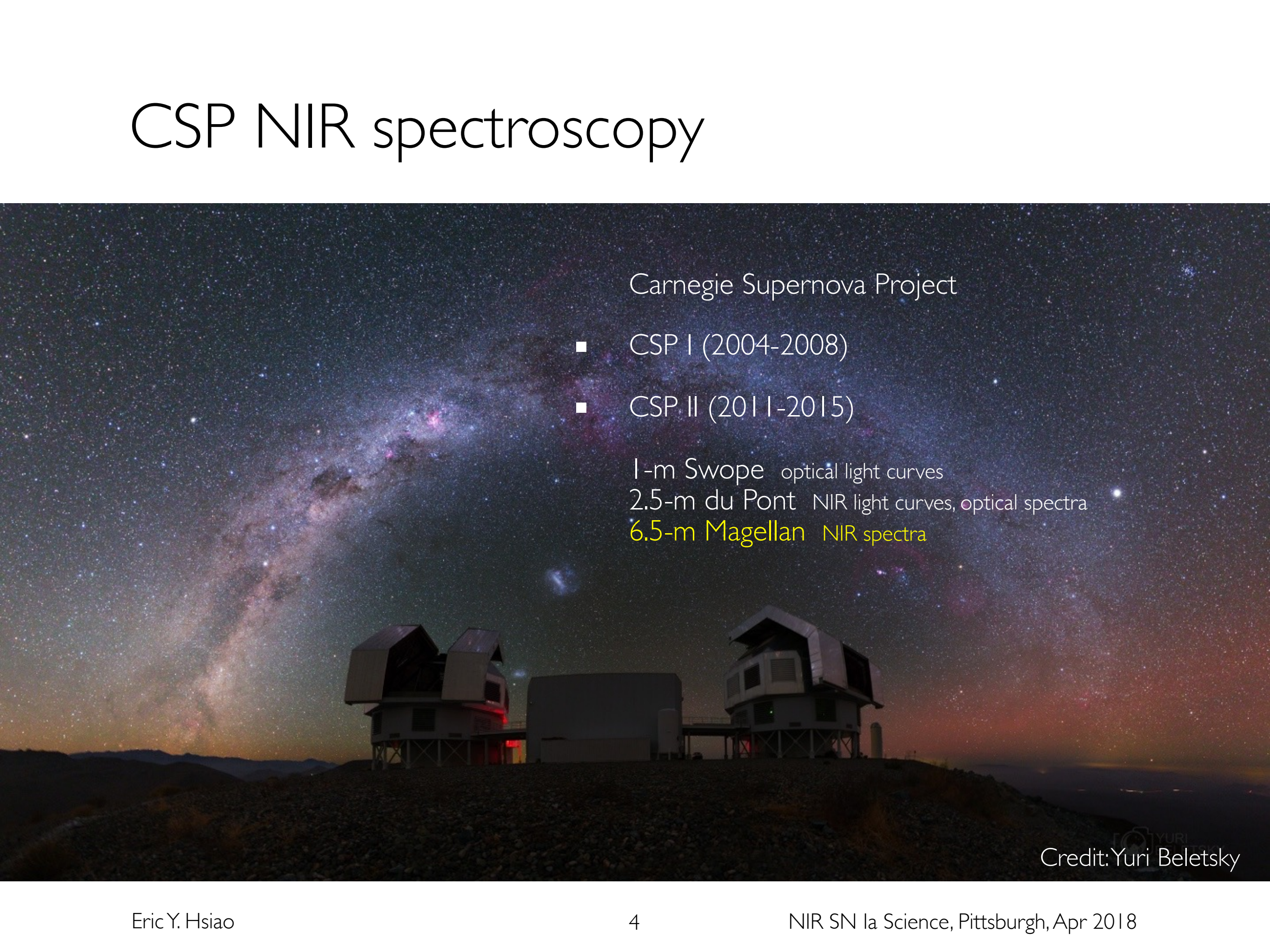


Credit: ESO

In the NIR, achieve higher precision in cosmology through 2 routes:

- By avoiding things we do not understand (shortcut)
- By constraining the physics (more fun!)

# CSP NIR spectroscopy



Carnegie Supernova Project

- CSP I (2004-2008)
- CSP II (2011-2015)

I-m Swope optical light curves  
2.5-m du Pont NIR light curves, optical spectra  
6.5-m Magellan NIR spectra

 Credit:Yuri Beletsky

# CSP NIR spectroscopy

- FIRE is the main workhorse of the project.
- In collaboration with CfA and Chilean institutions, we obtained a total of 70+ nights on Magellan. That is approximately 1 night per week during Chilean summer.
- ToO resources fill in the gap.
- High-throughput prism mode,  $R=500$  at J.

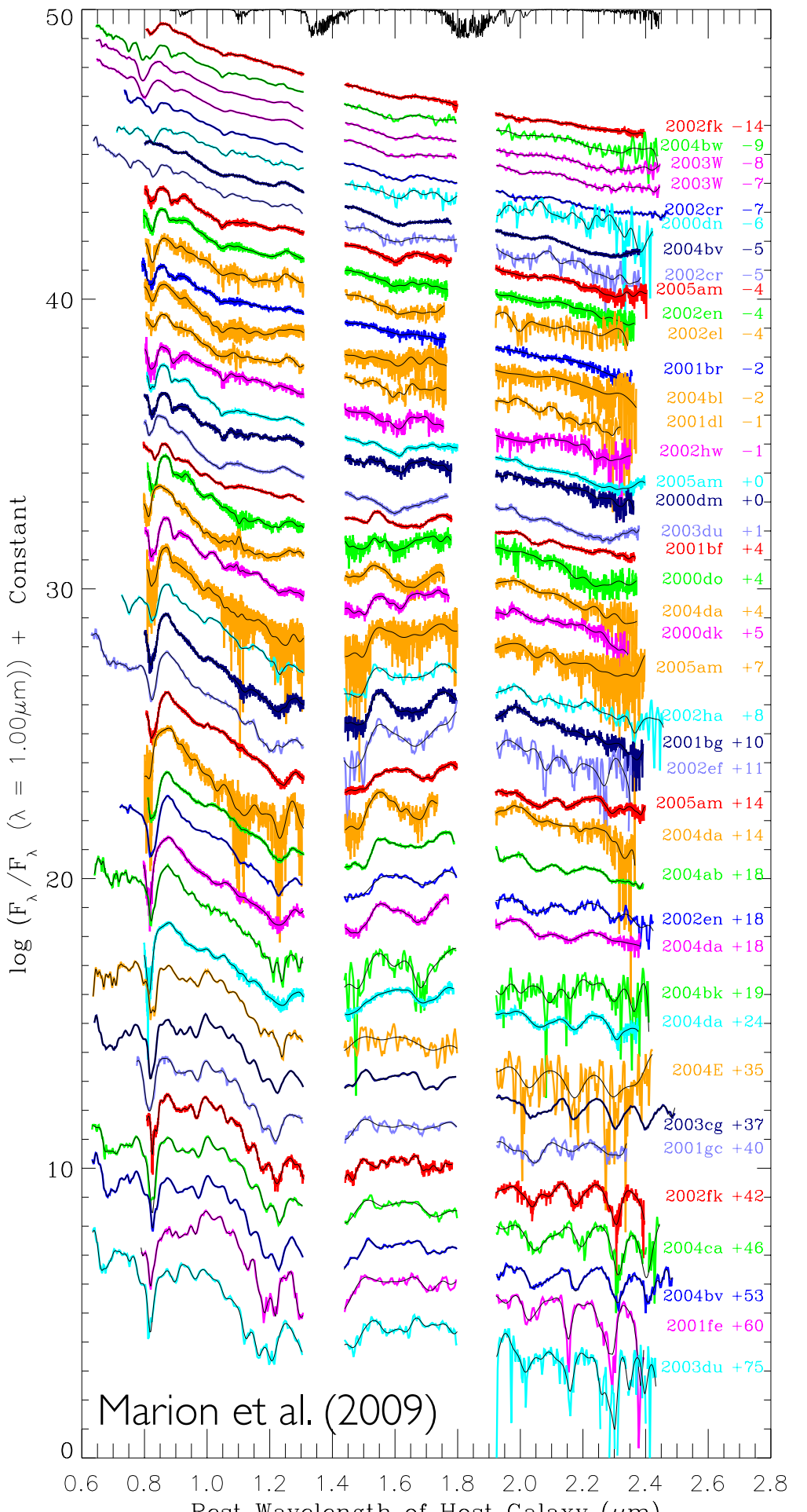


Credit:Yuri Beletsky 

# CSP NIR spectroscopy

Improvements over previous largest SN Ia sample (Marion et al. 2009)

- Larger sample
- Time-series observations
- Complementary LCs
- Simultaneous optical spectra
- Improved telluric region

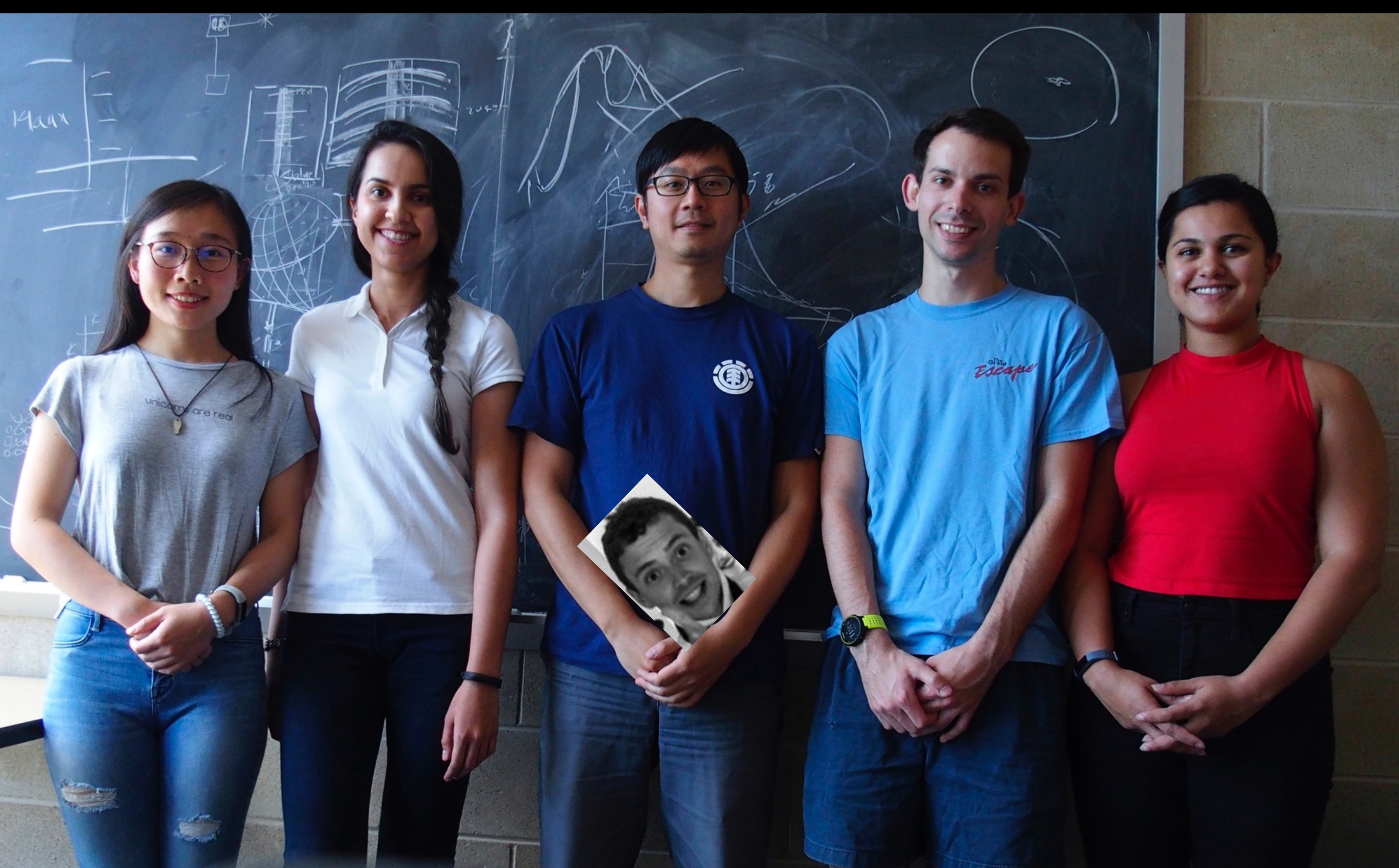


# CSP NIR spectroscopy

Table 1. Number of NIR spectra by instrument and supernova type

Telescope	Instrument	Ia	Iax	Ibc	II	IIIn	SLSN	Others	Total
Magellan Baade	FIRE	459	27	101	81	35	9	4	716
Gemini North	GNIRS	58	7	0	0	0	0	0	65
IRTF	SpeX	40	2	6	9	1	0	0	58
Mt Abu	NICS	31	0	0	0	0	0	0	31
Gemini South	FLAMINGOS2	17	0	0	1	0	0	0	18
Magellan Clay	MMIRS	7	1	2	1	0	0	1	12
VLT	ISAAC	8	4	0	0	0	0	0	12
NTT	SofI	4	1	2	0	0	0	0	7
Total spectra		624	42	111	92	36	9	5	919
Total SNe		151	9	44	33	11	5	2	255

Hsiao et al. in prep



Jing  
Lu

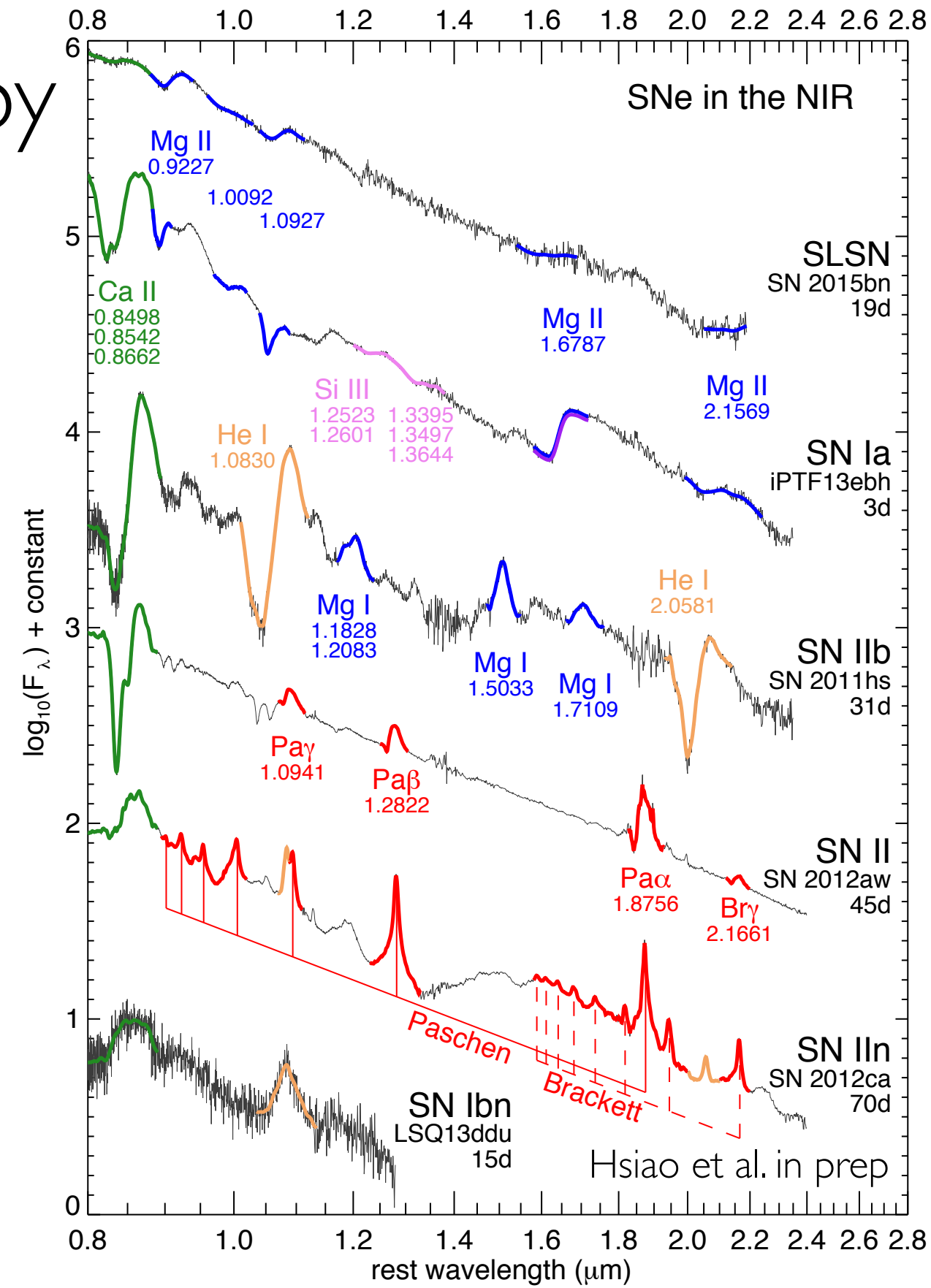
Melissa  
Shahbandeh

Scott  
Davis

Sahana  
Kumar

# CSP NIR spectroscopy

- Stronger, more isolated lines in the NIR compared to optical.
- NIR probes different depths in the ejecta.
- Brackett, Paschen lines constrain level populations.
- 2 strong NIR He I lines.



# Type Ia NIR spectra

## Sample characteristics

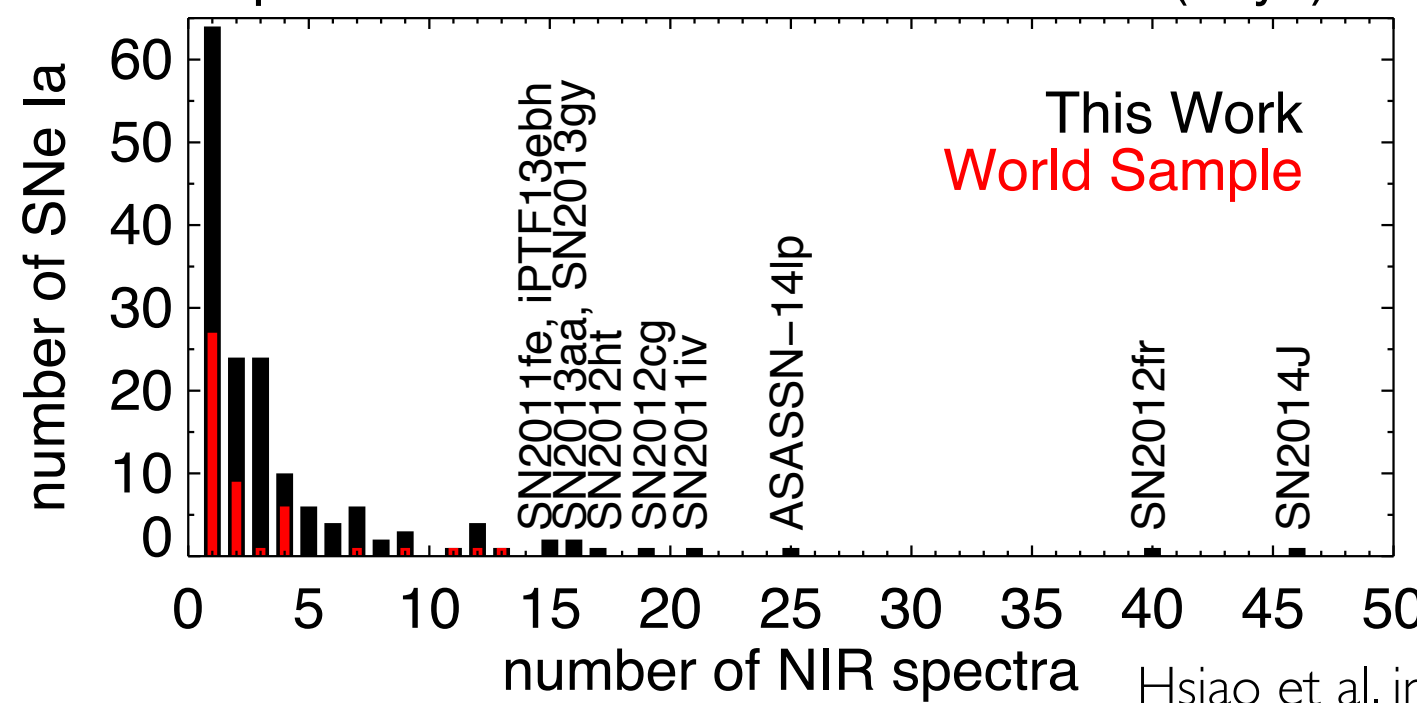
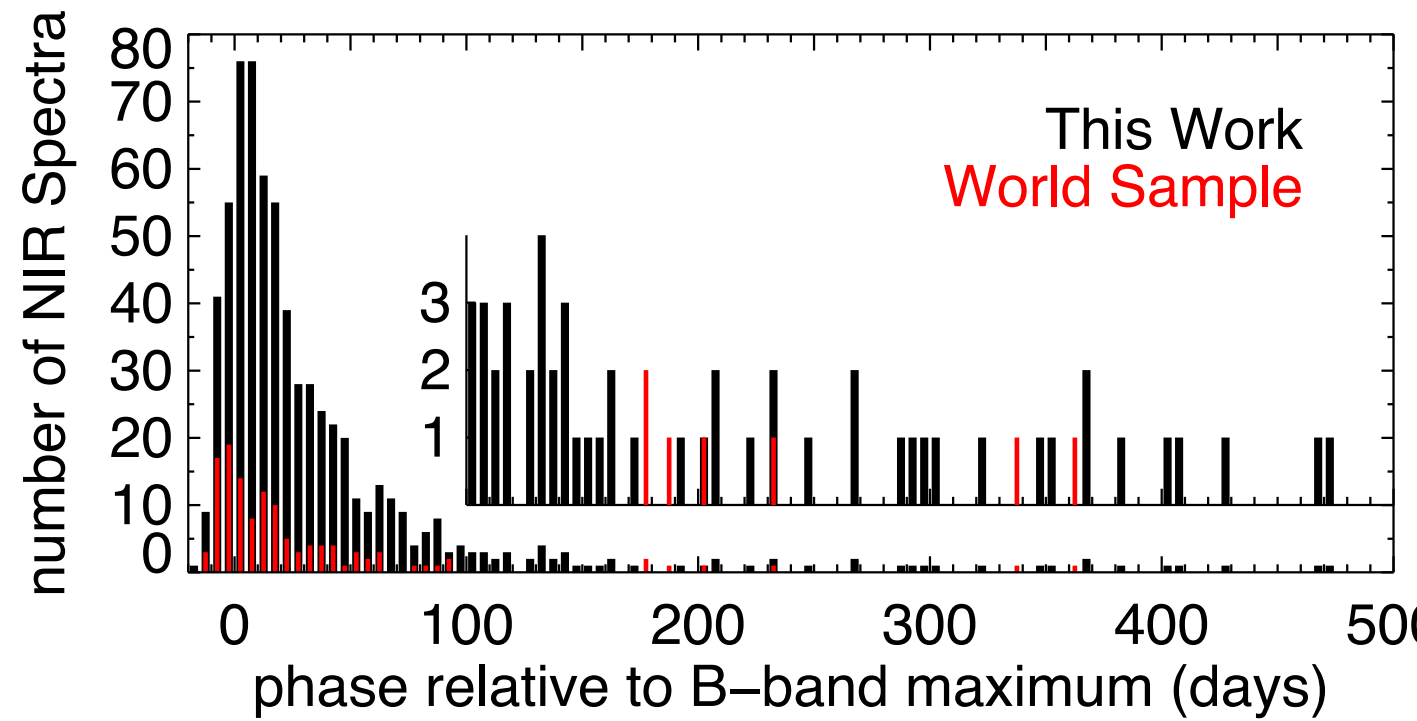
Table 1. Number of NIR spectra by instrument and supernova type

Telescope	Instrument	Ia	Iax	Ibc	II	IIIn	SLSN	Others	Total
Magellan Baade	FIRE	459	27	101	81	35	9	4	716
Gemini North	GNIRS	58	7	0	0	0	0	0	65
IRTF	SpeX	40	2	6	9	1	0	0	58
Mt Abu	NICS	31	0	0	0	0	0	0	31
Gemini South	FLAMINGOS2	17	0	0	1	0	0	0	18
Magellan Clay	MMIRS	7	1	2	1	0	0	1	12
VLT	ISAAC	8	4	0	0	0	0	0	12
NTT	SofI	4	1	2	0	0	0	0	7
Total spectra		624	42	111	92	36	9	5	919
Total SNe		151	9	44	33	11	5	2	255

Hsiao et al. in prep

# Type Ia NIR spectra

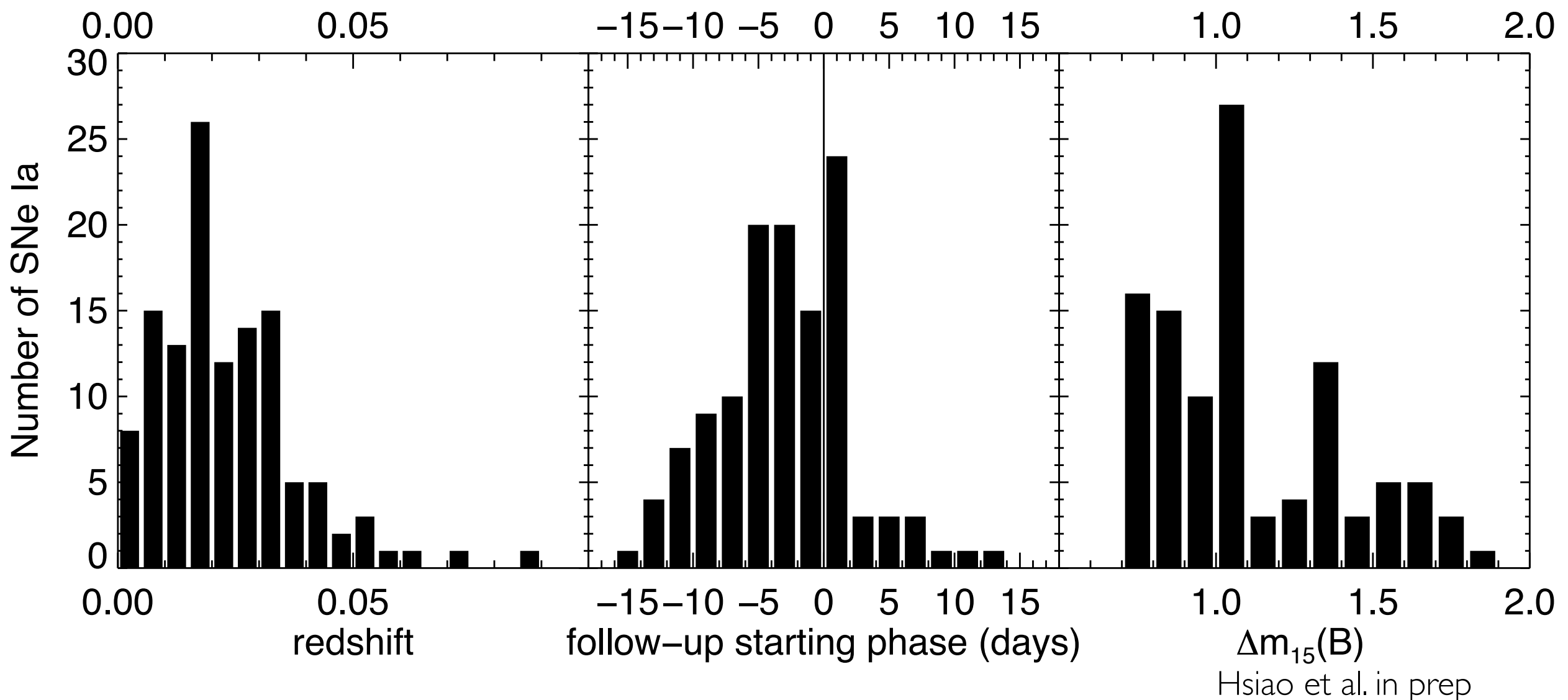
## Sample characteristics



Hsiao et al. in prep

# Type Ia NIR spectra

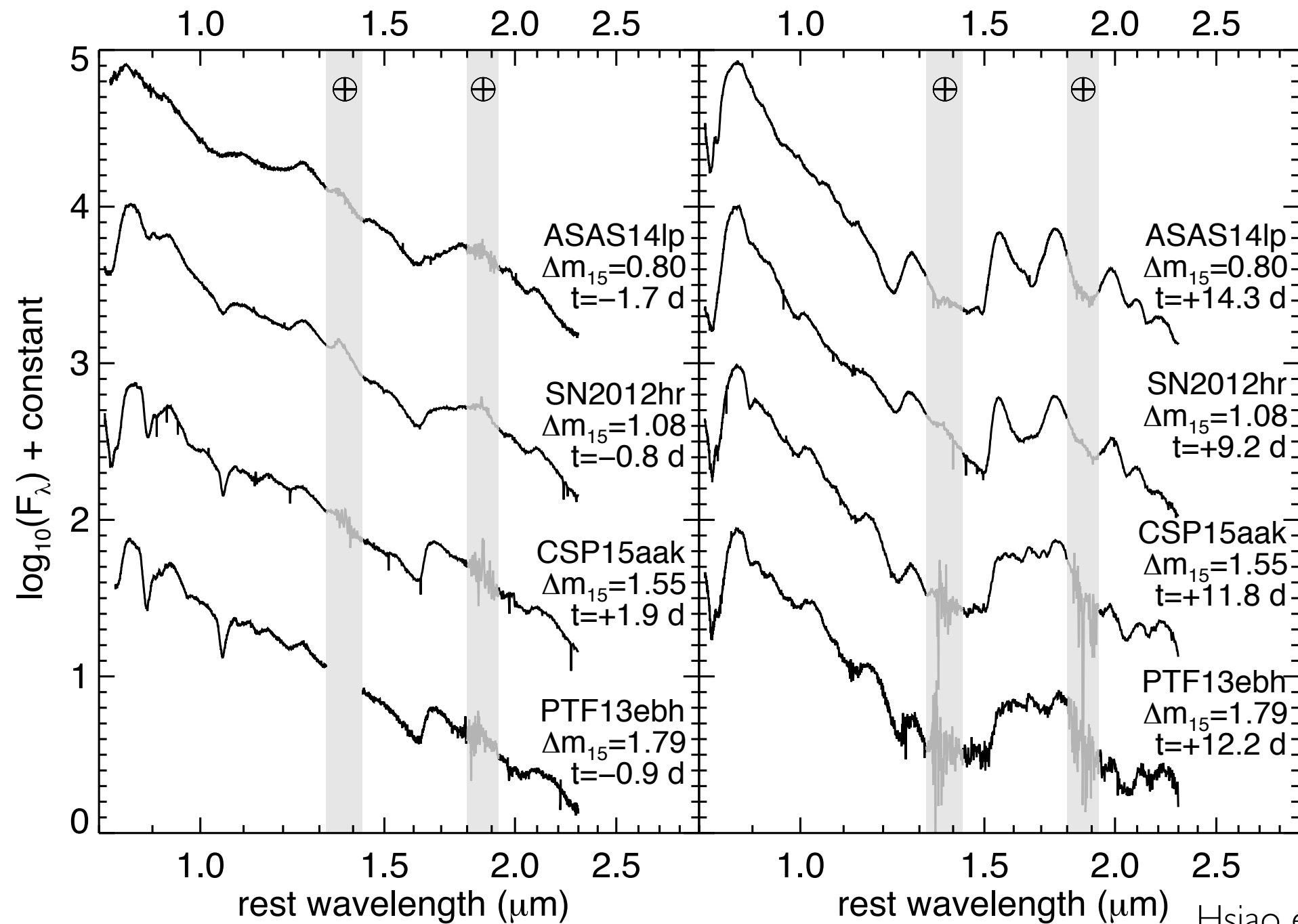
Sample characteristics



Hsiao et al. in prep

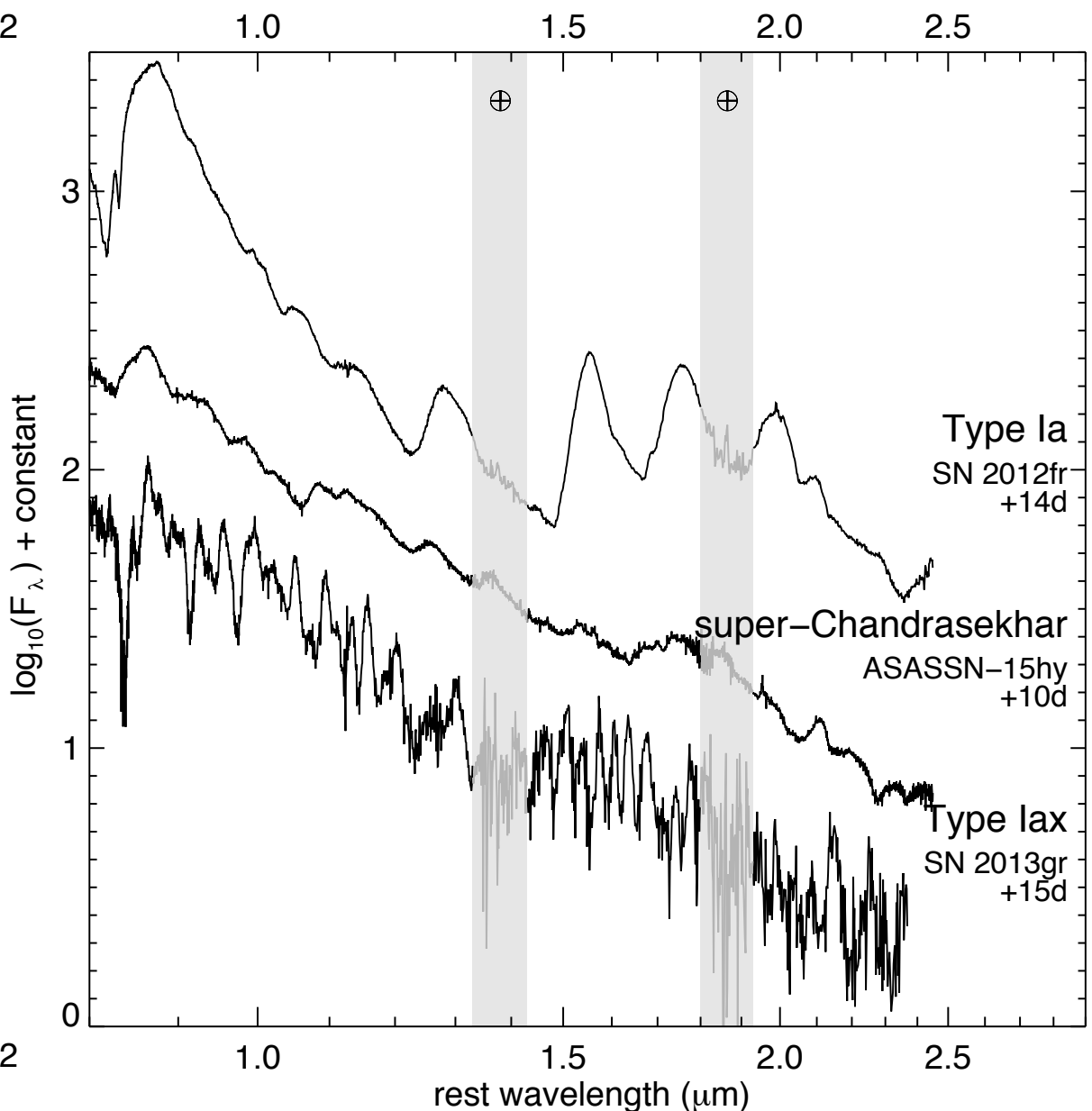
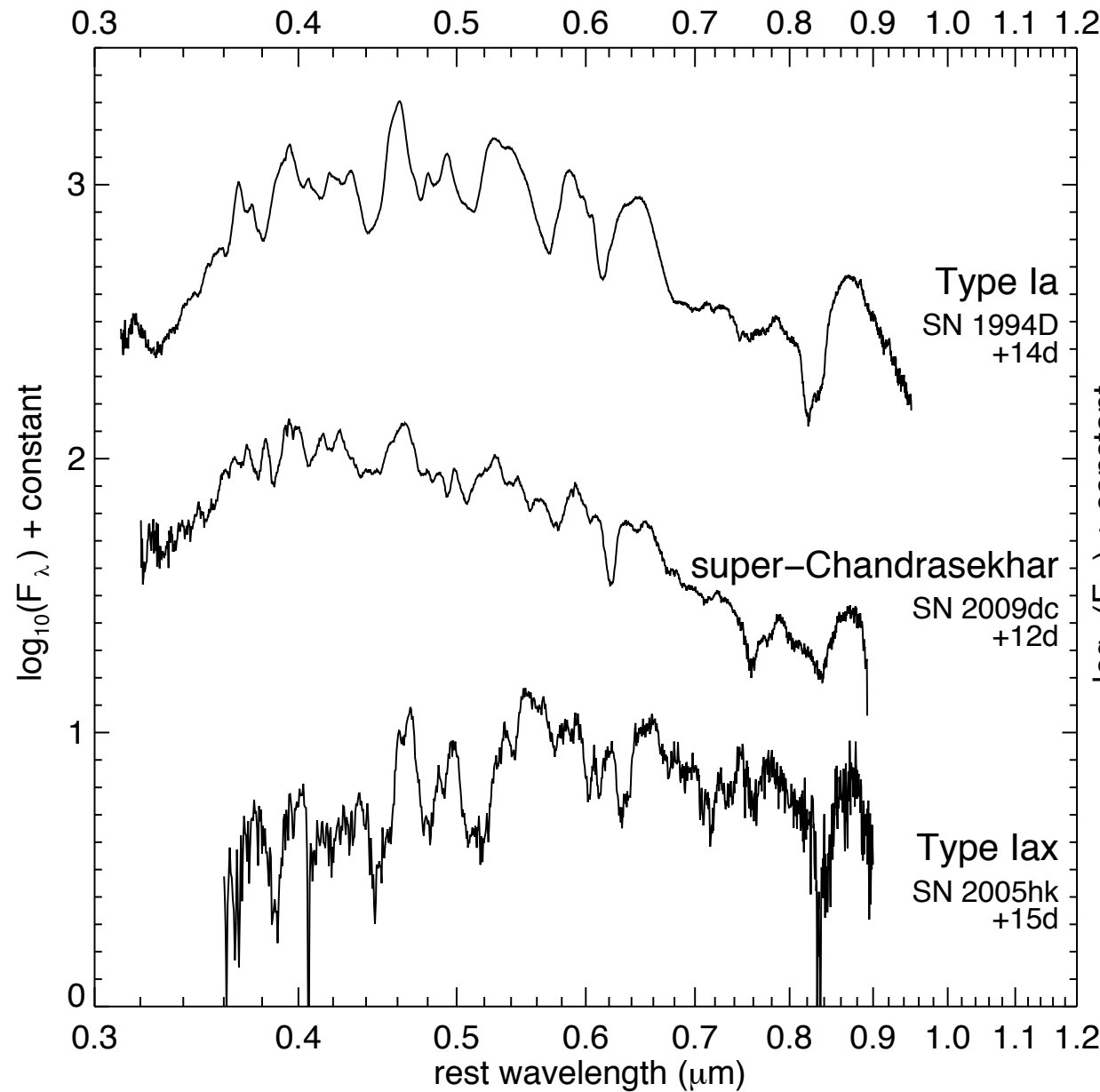
# Type Ia NIR spectra

K-corrections



# Type Ia NIR spectra

Peculiar objects

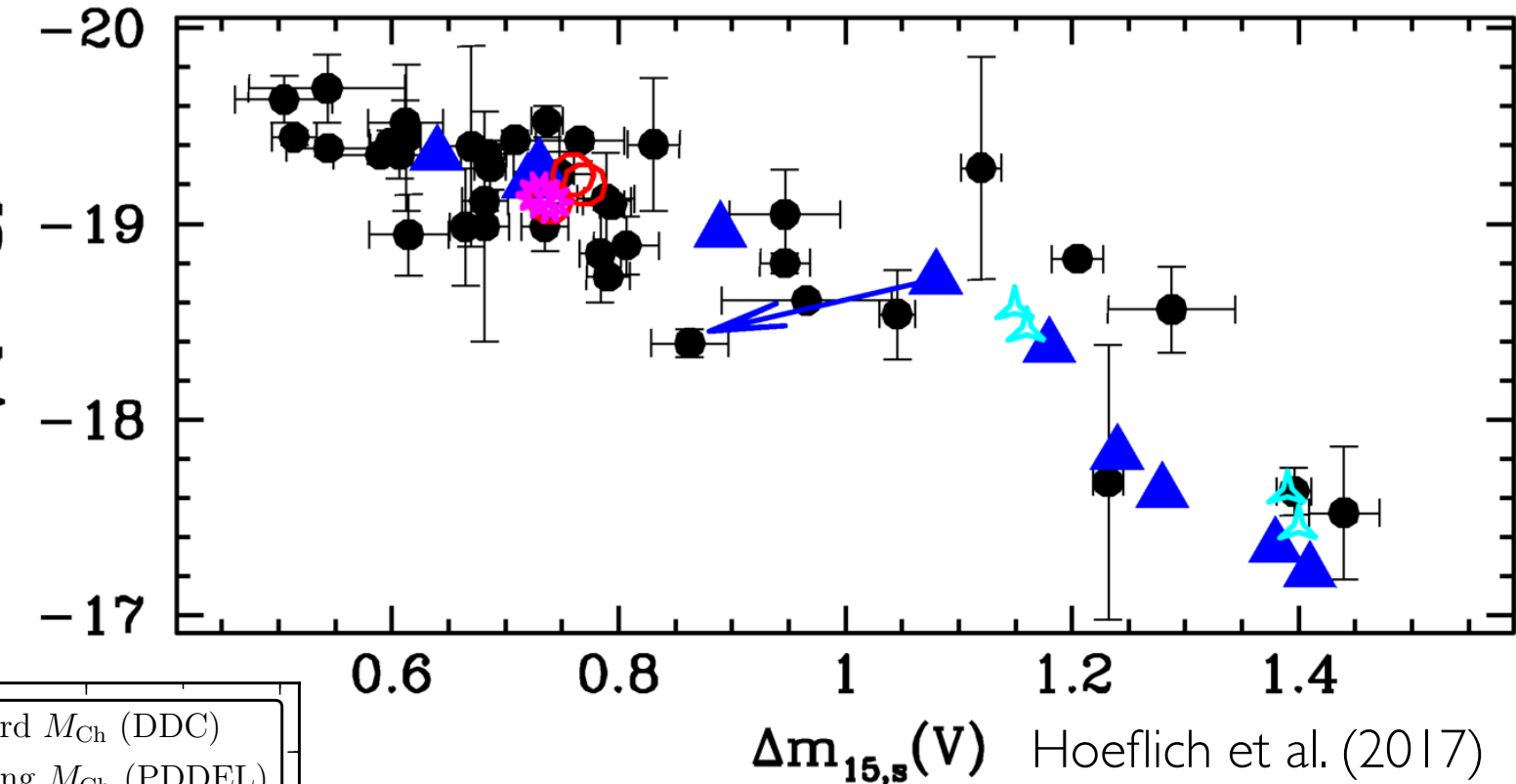
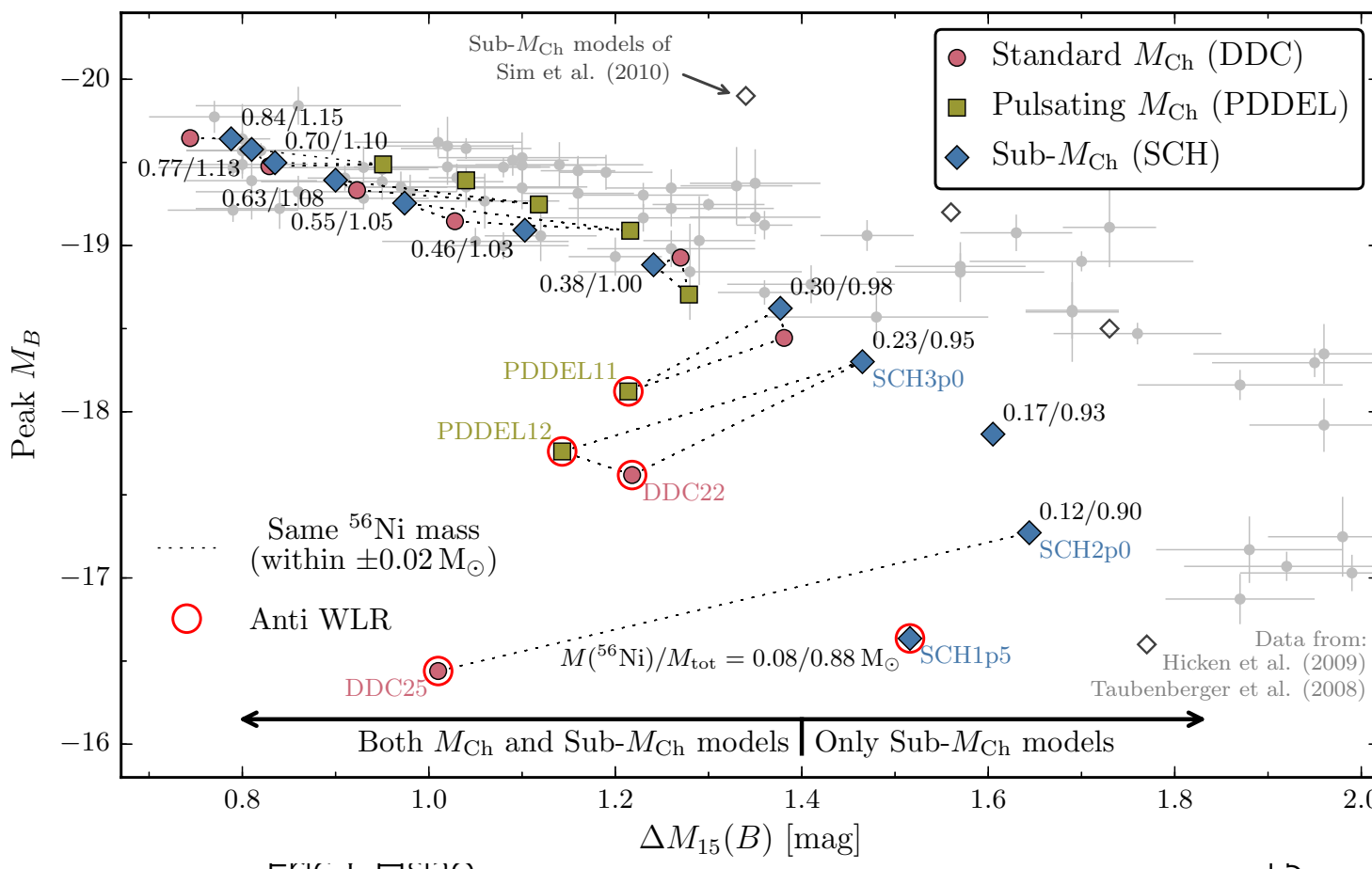


Hsiao et al. in prep

# Probing SN Ia physics

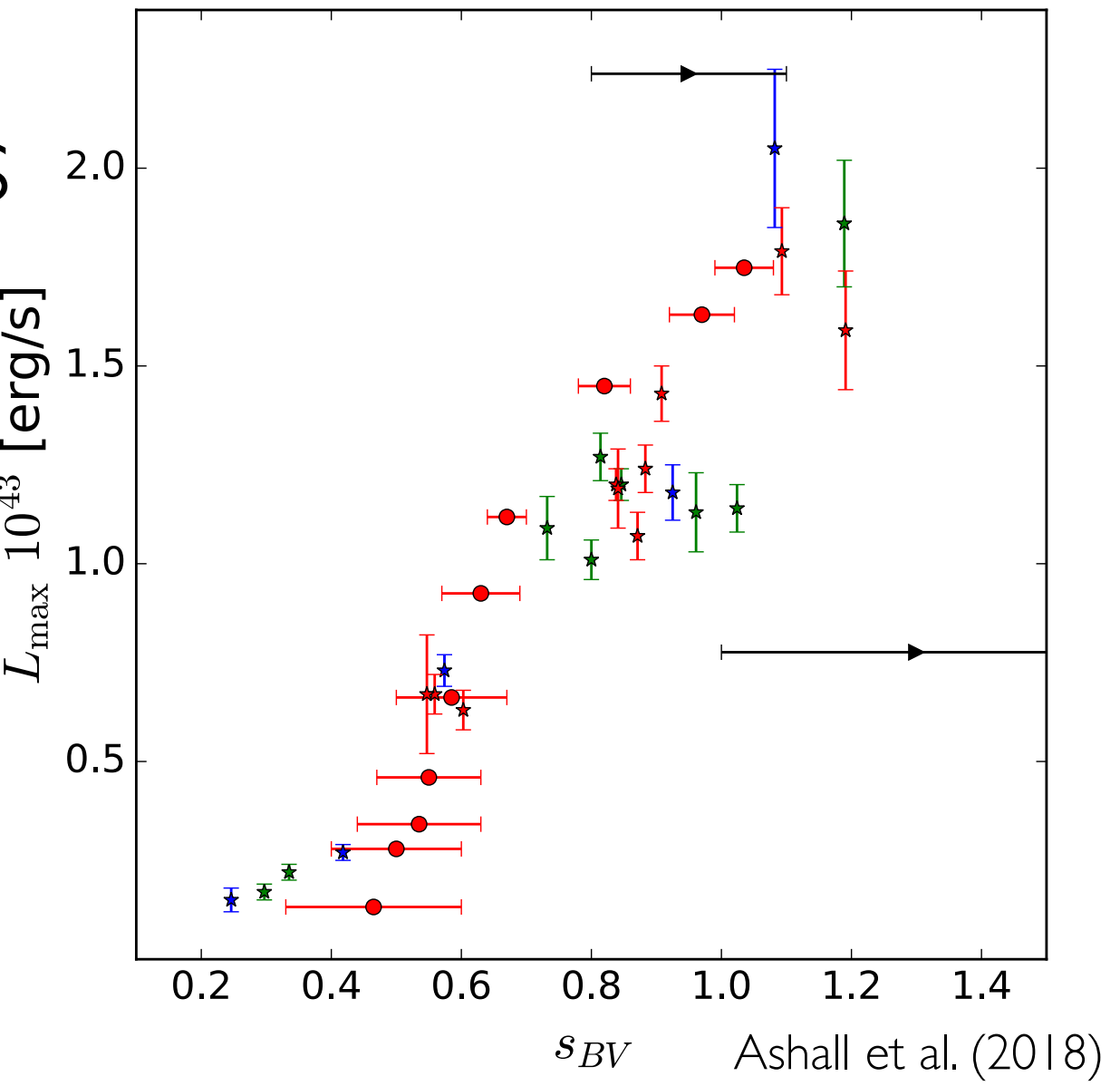
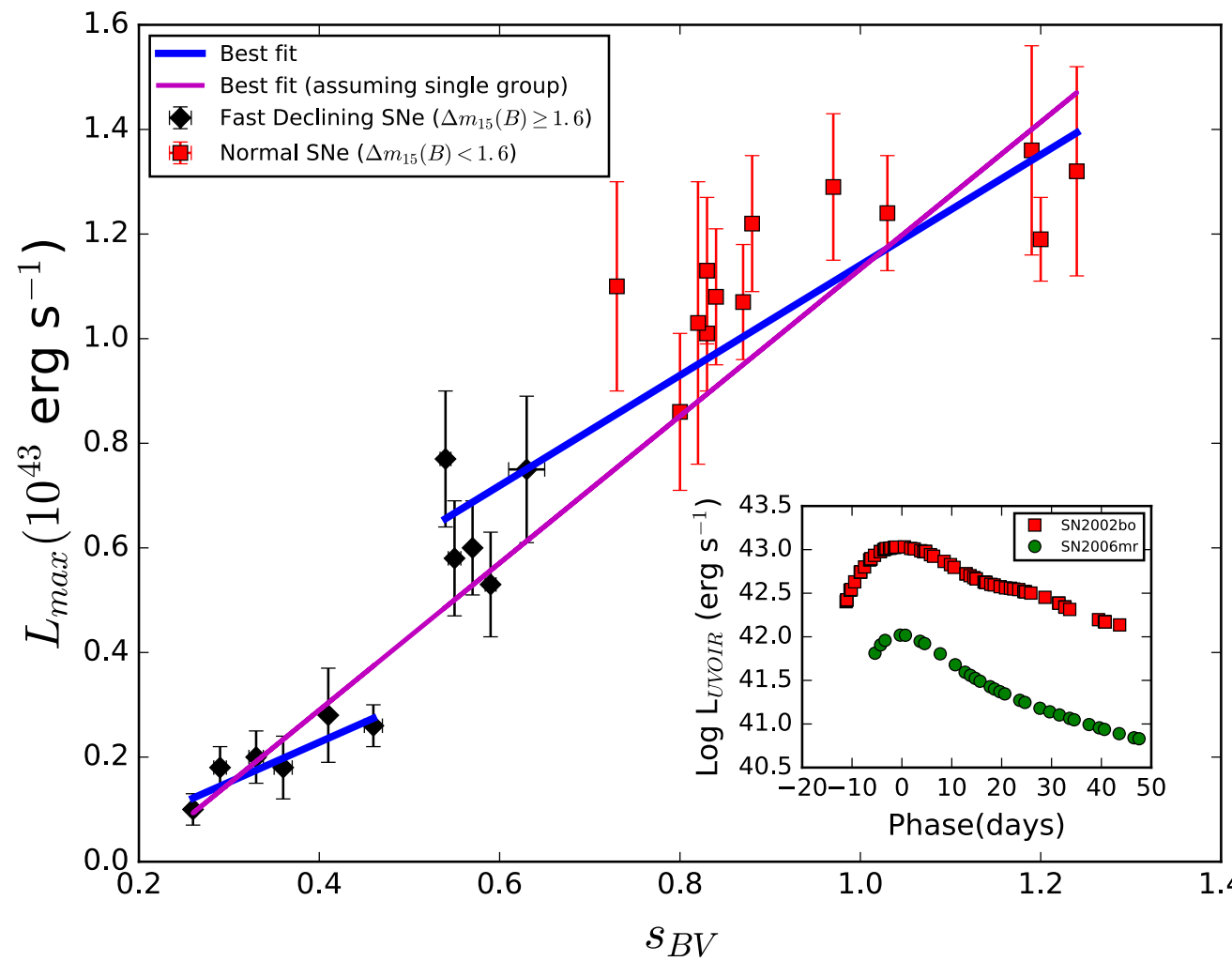
- Is the normal SN Ia population composed of a single or multiple triggering mechanisms?
- Chandrasekhar-mass or sub-Chandrasekhar-mass trigger?

Blondin et al. (2017)



# Probing SN Ia physics

- Is the normal SN Ia population composed of a single or multiple triggering mechanisms?
- Chandrasekhar-mass or sub-Chandrasekhar-mass trigger?



Ashall et al. (2018)

Dhawan et al. (2017)

# Probing SN Ia physics

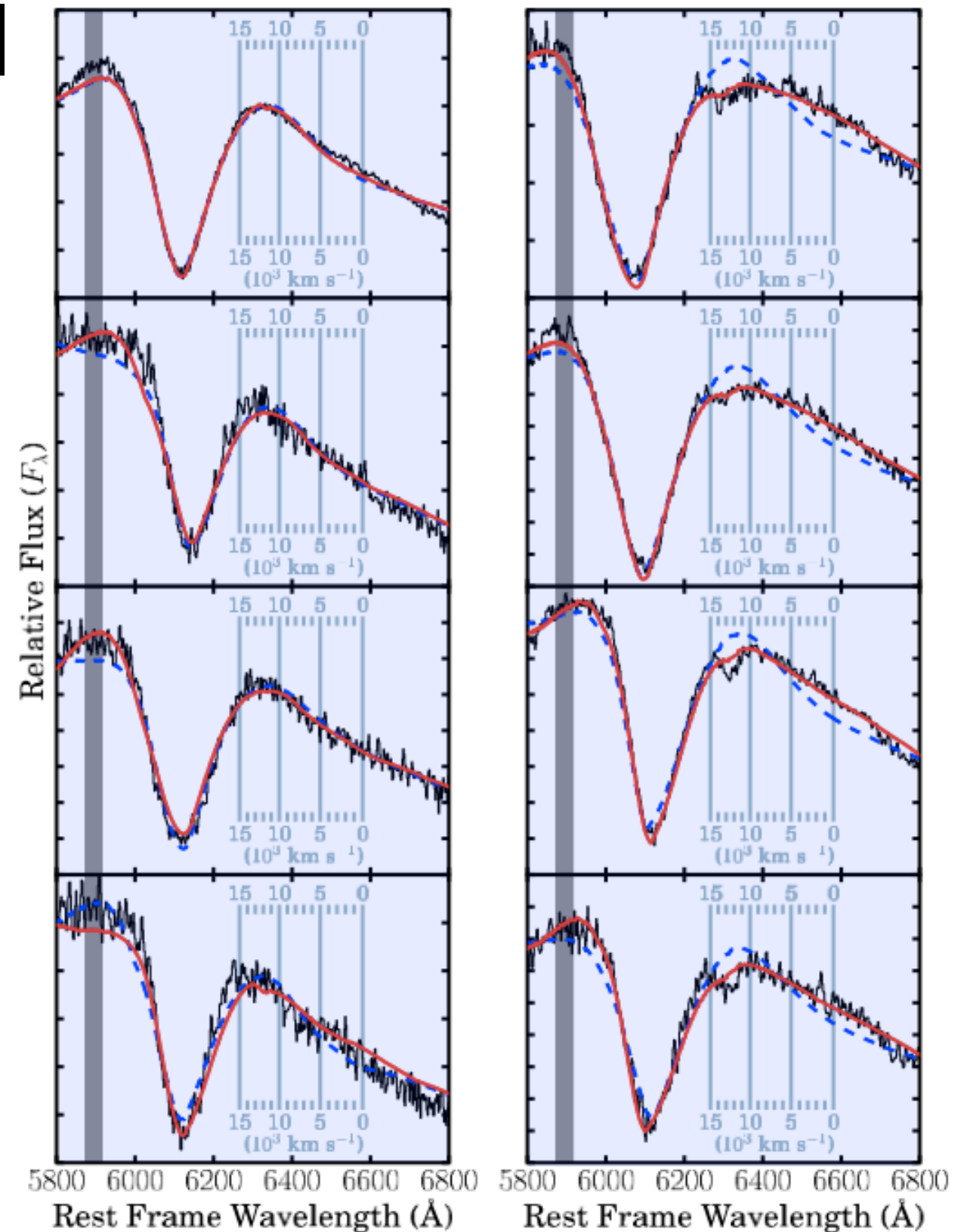
- Unburned material  
*Premax C I 1.069, He I 1.083*  
Marion et al. (2006), Hsiao et al. (2013, 2015)
- Boundary between C/O burning  
*Premax Mg II 1.093*  
Wheeler et al. (1998), Hsiao et al. (2013)
- Radioactive nickel, ionization evolution  
*Postmax H-band break*  
Wheeler et al. (1998), Hoeflich et al. (2002), Hsiao et al. (2013)
- Stable nickel  
*Transitional phase [Ni II] 1.939*  
Friesen et al. (2014), Wilk et al. (2018)
- Companion signature  
*Postmax P-beta 1.282*  
Maeda et al. (2014), Sand et al. (2016), Botyanszki (2017)
- Central density and B-field  
*Nebular phase [Fe II] 1.644*  
Penney & Hoeflich (2014), Diamond et al. (2015), Diamond et al. (2018)

# Unburned material

Premax C I I.069, He I I.083

- Carbon: pristine material from the progenitor
- Incomplete burning: constraints for explosion models
- Optical C II 6580 detected in 20-30% of SNe Ia

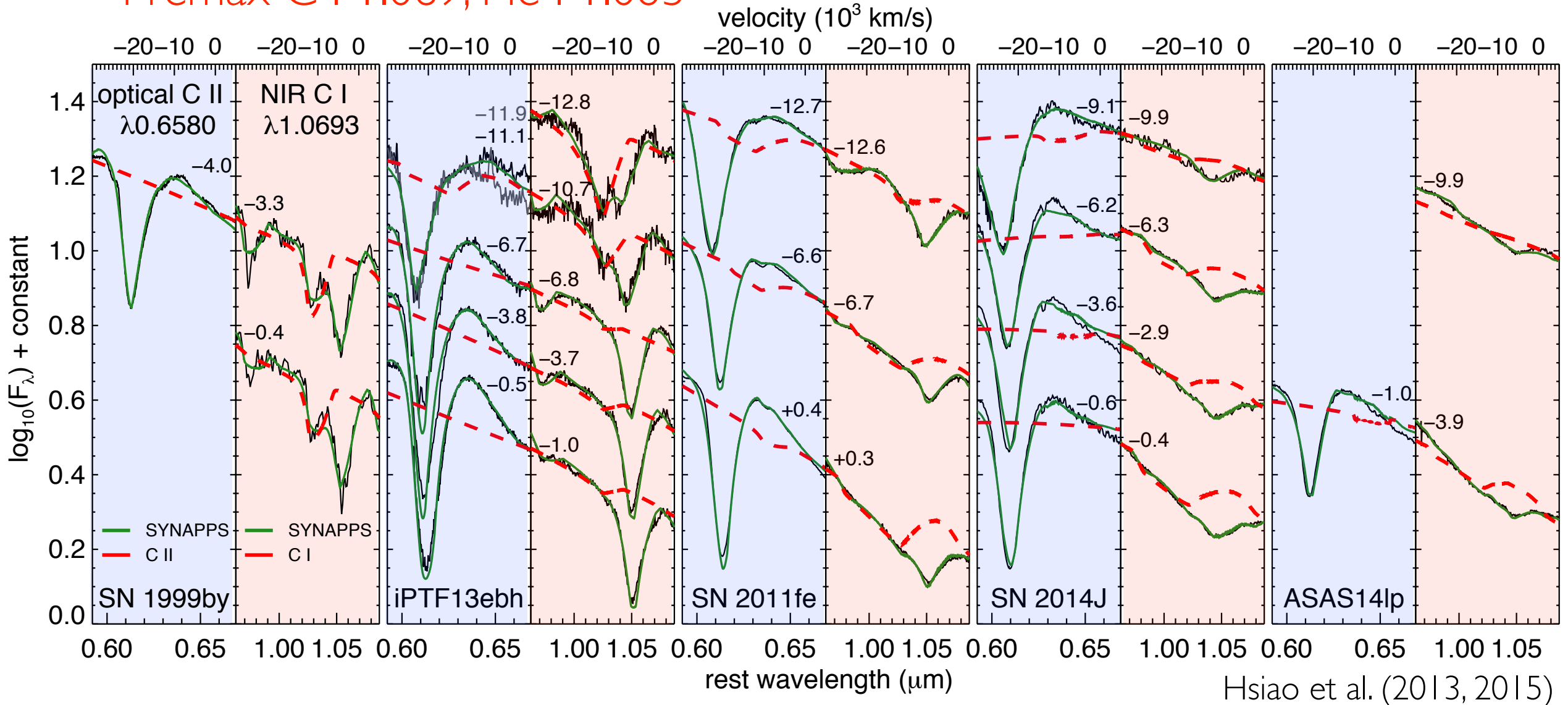
Thomas et al. (2011)  
Folatelli et al. (2012)  
Silverman et al. (2012)



Thomas et al. (2011)

# Unburned material

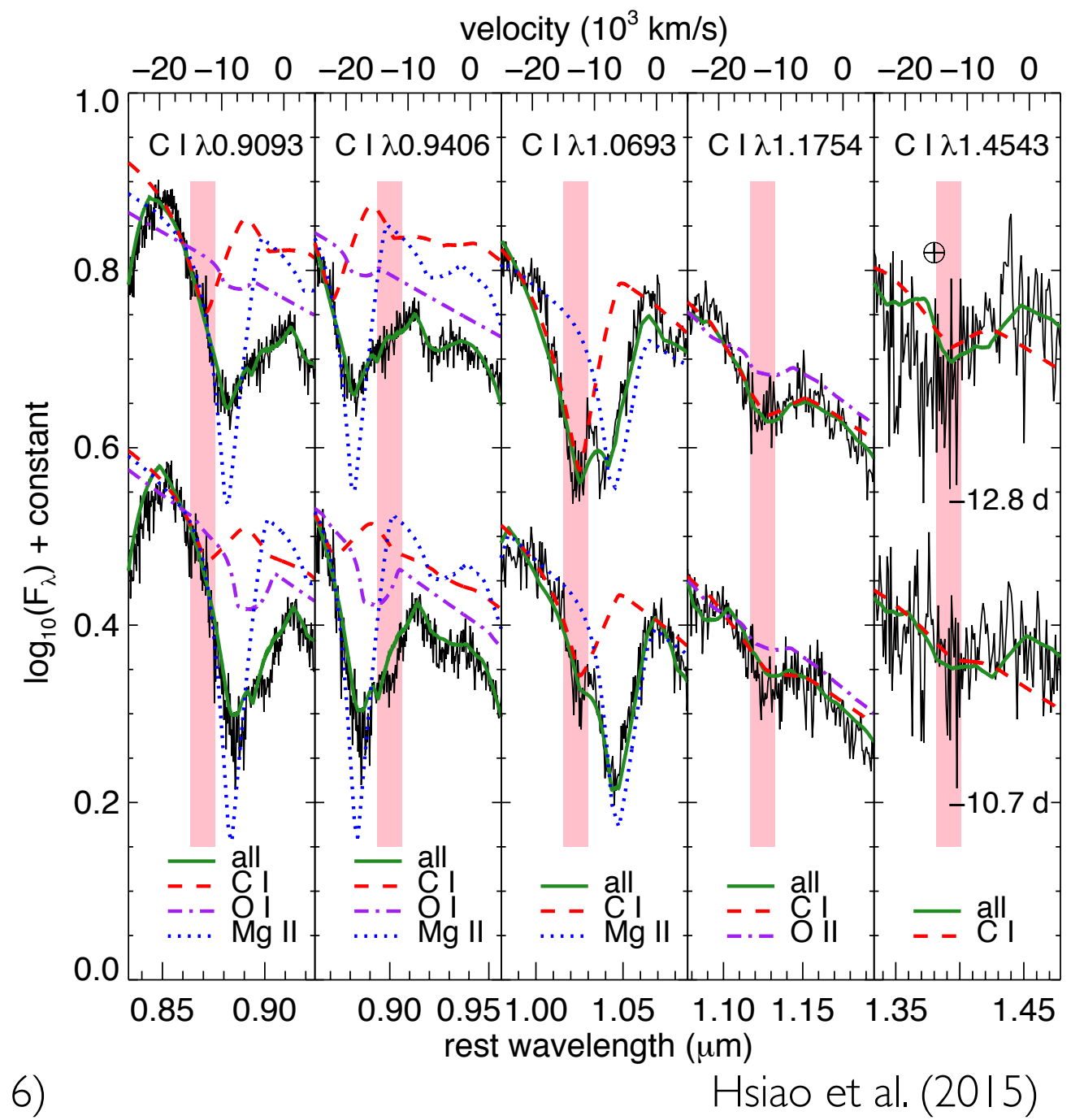
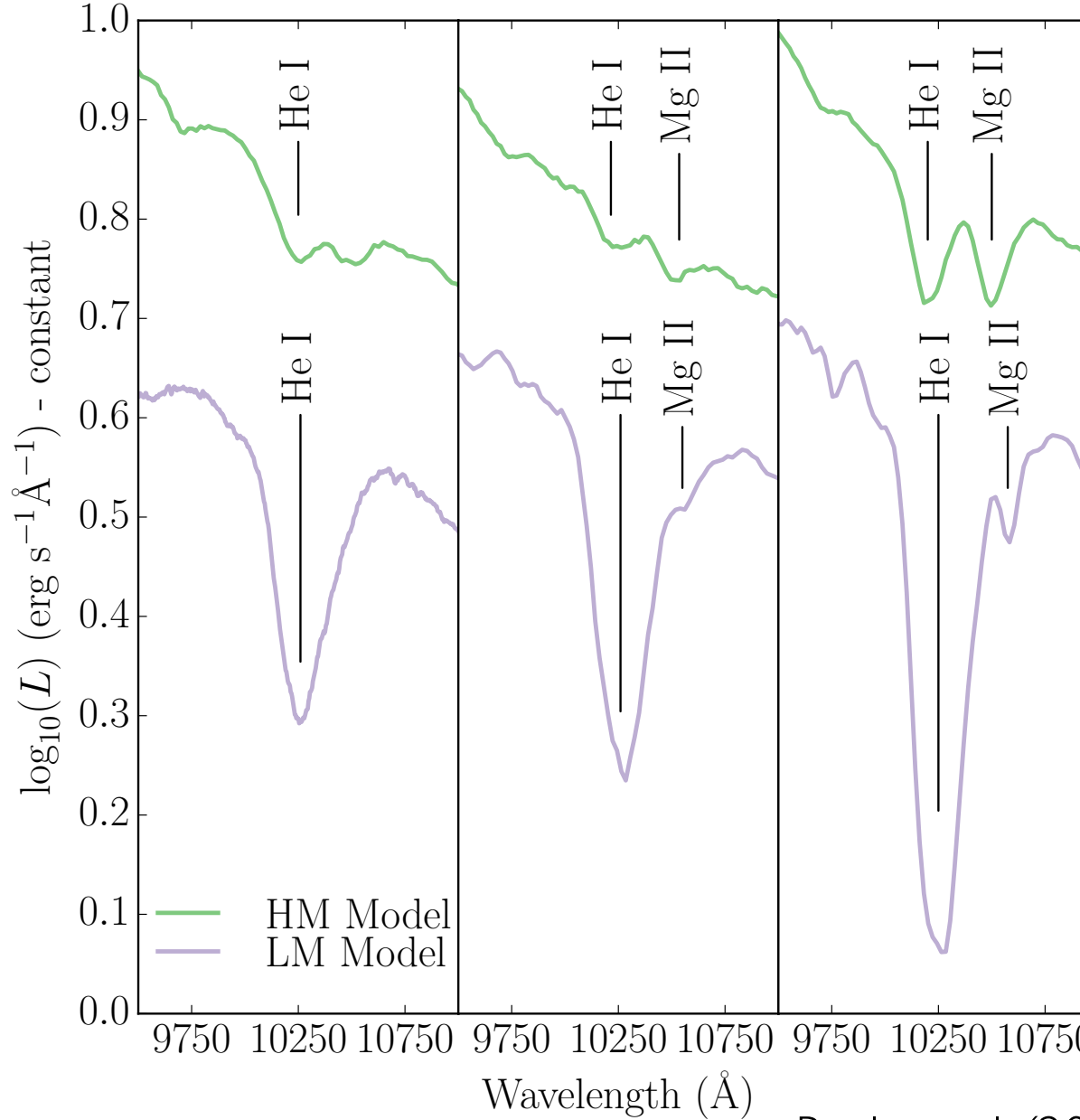
Premax C I I.069, He I I.083



- NIR provides a more complete census of carbon than the optical
- Unburned carbon appears to be ubiquitous.
- Carbon detection is inconsistent with He detonation.

# Unburned material

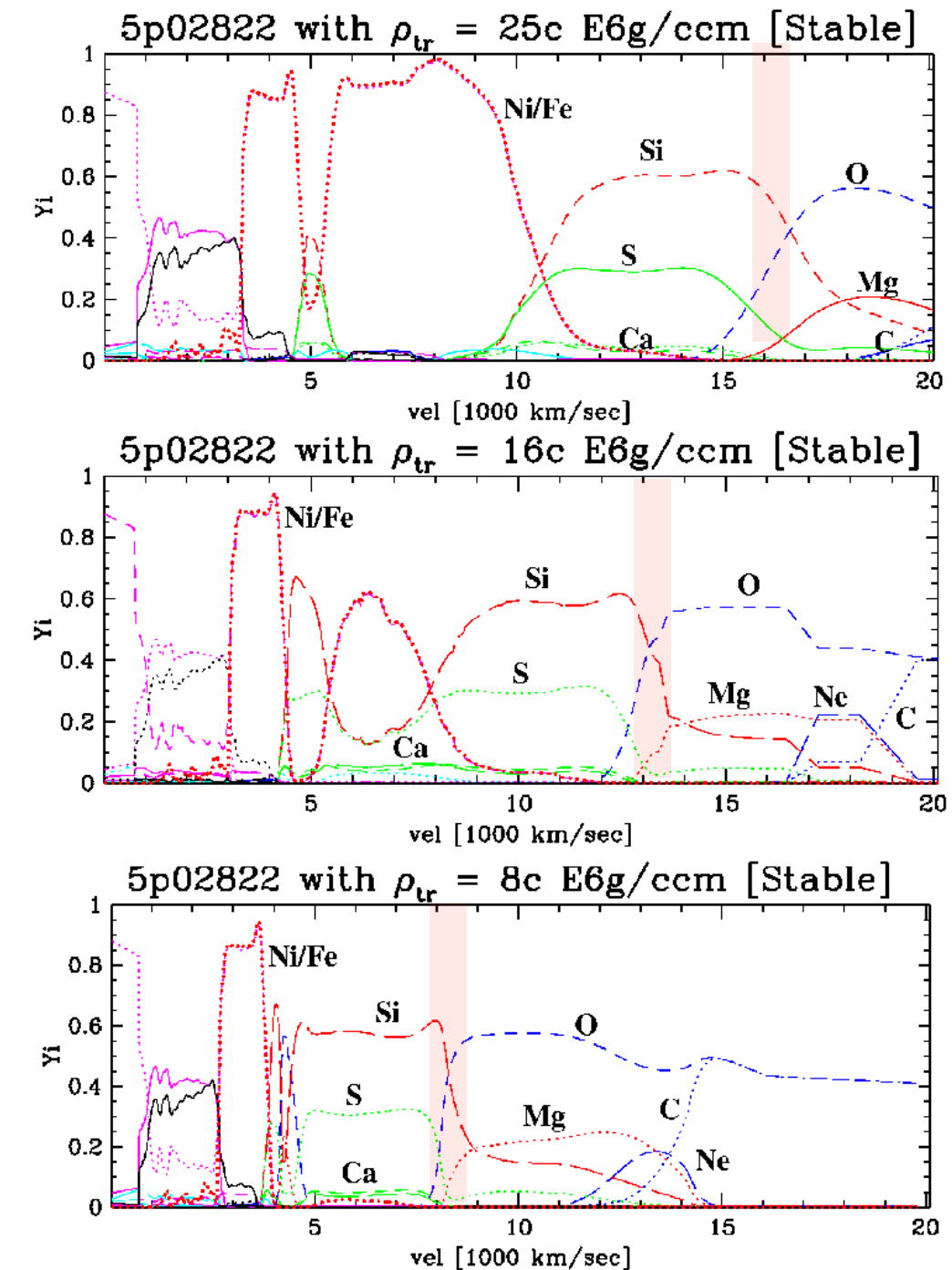
Premax C I 1.069, He I 1.083



# Boundary between C/O burning

Premax Mg II 1.093

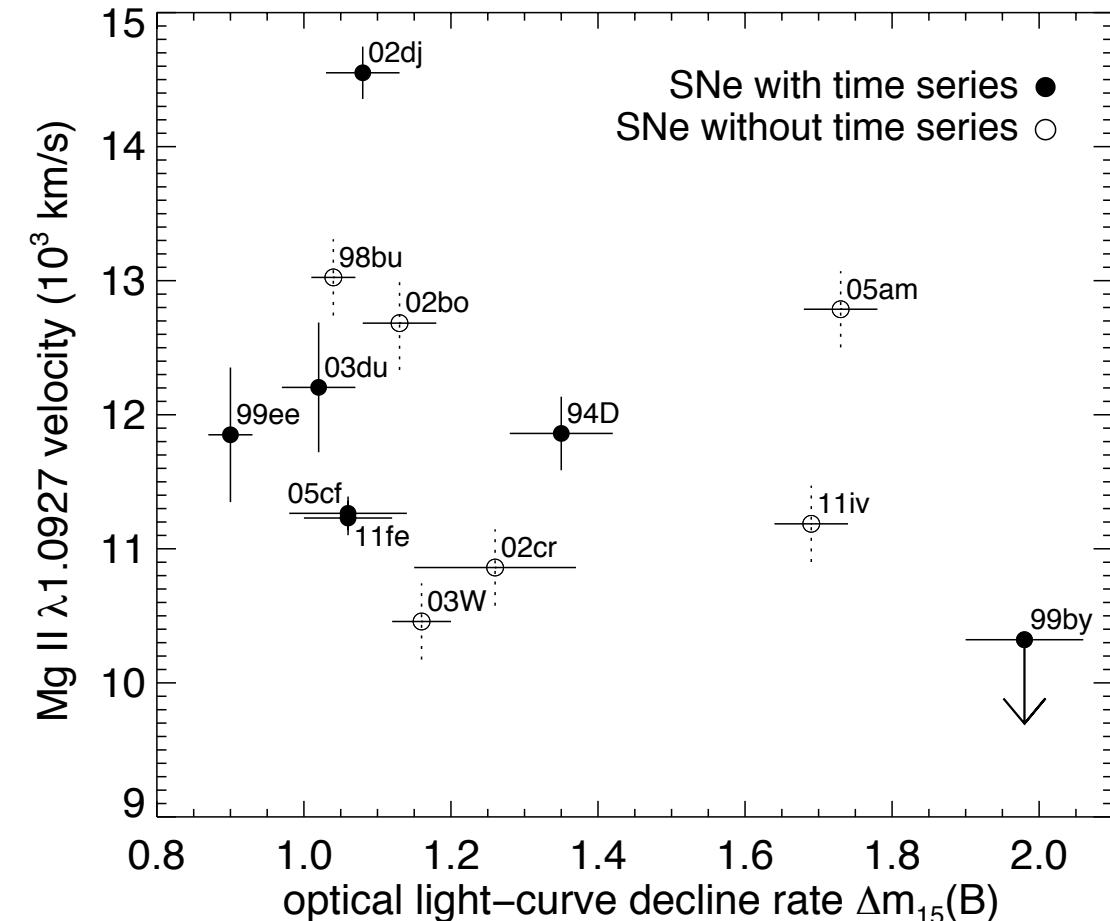
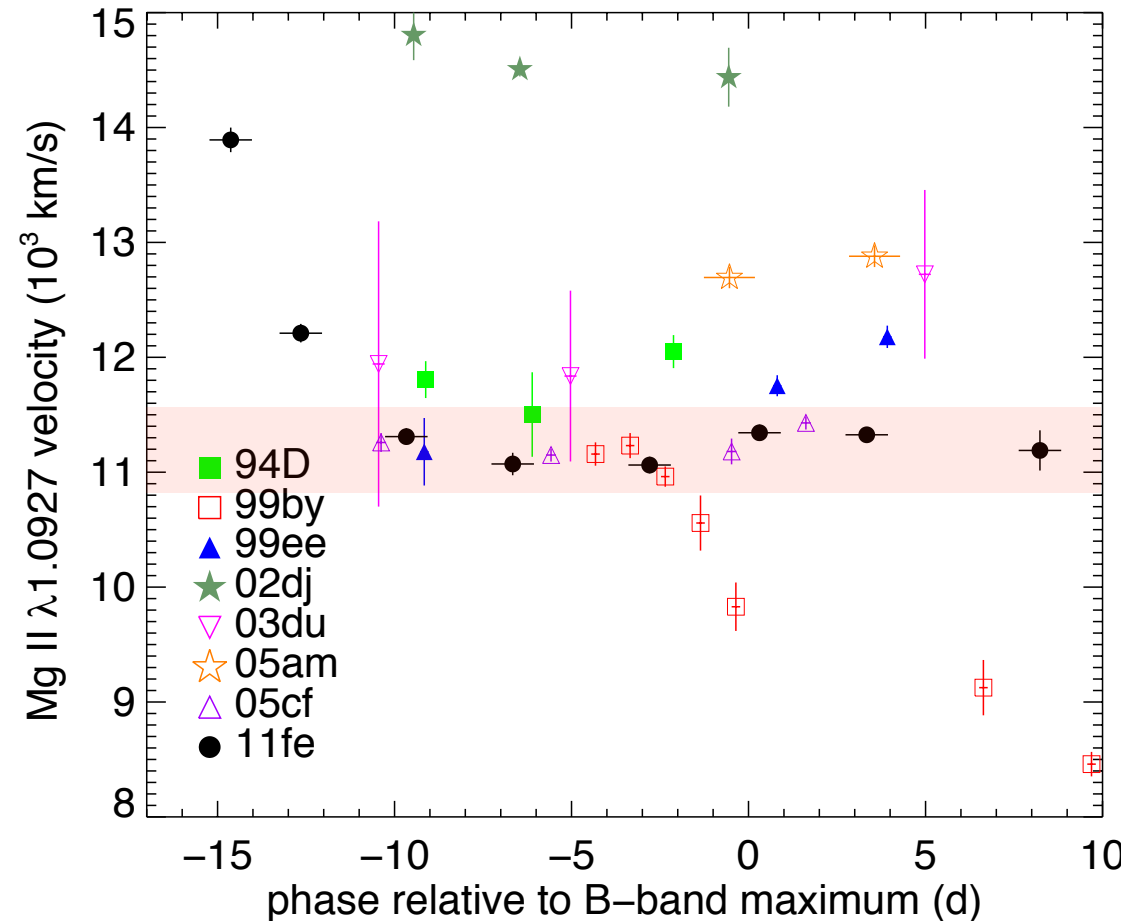
- Mg II: strong, isolated line
- Flat Mg velocity evolution: bottom of C burning layer
- Boundary between C/O burning
- Sensitive to transition density



Wheeler et al. (1998), Höflich et al. (2002)

# Boundary between C/O burning

Premax Mg II 1.093

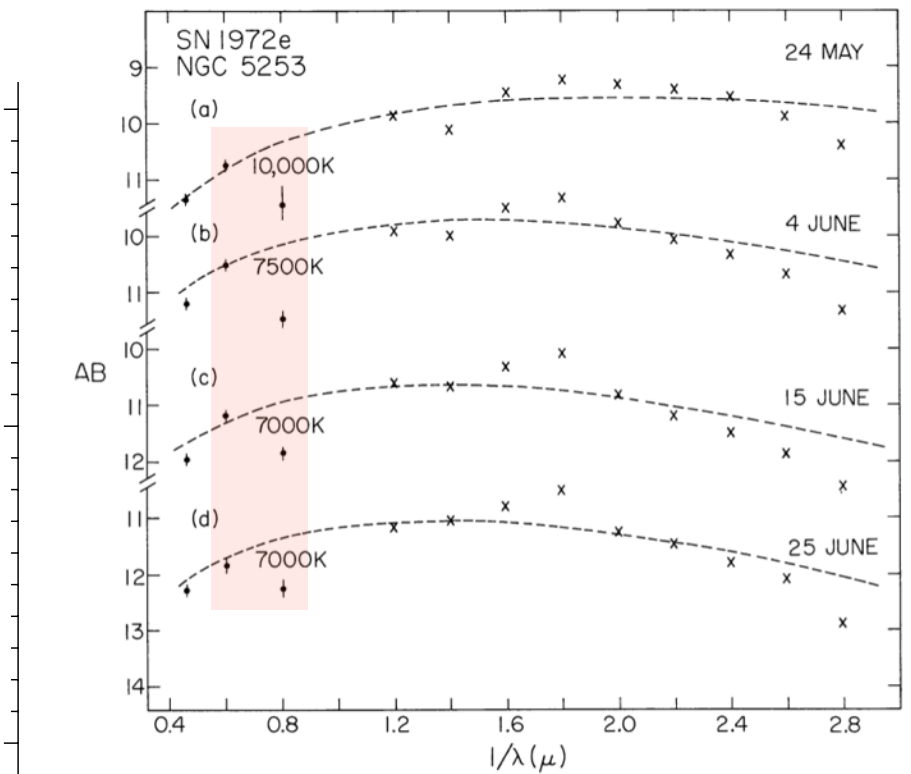
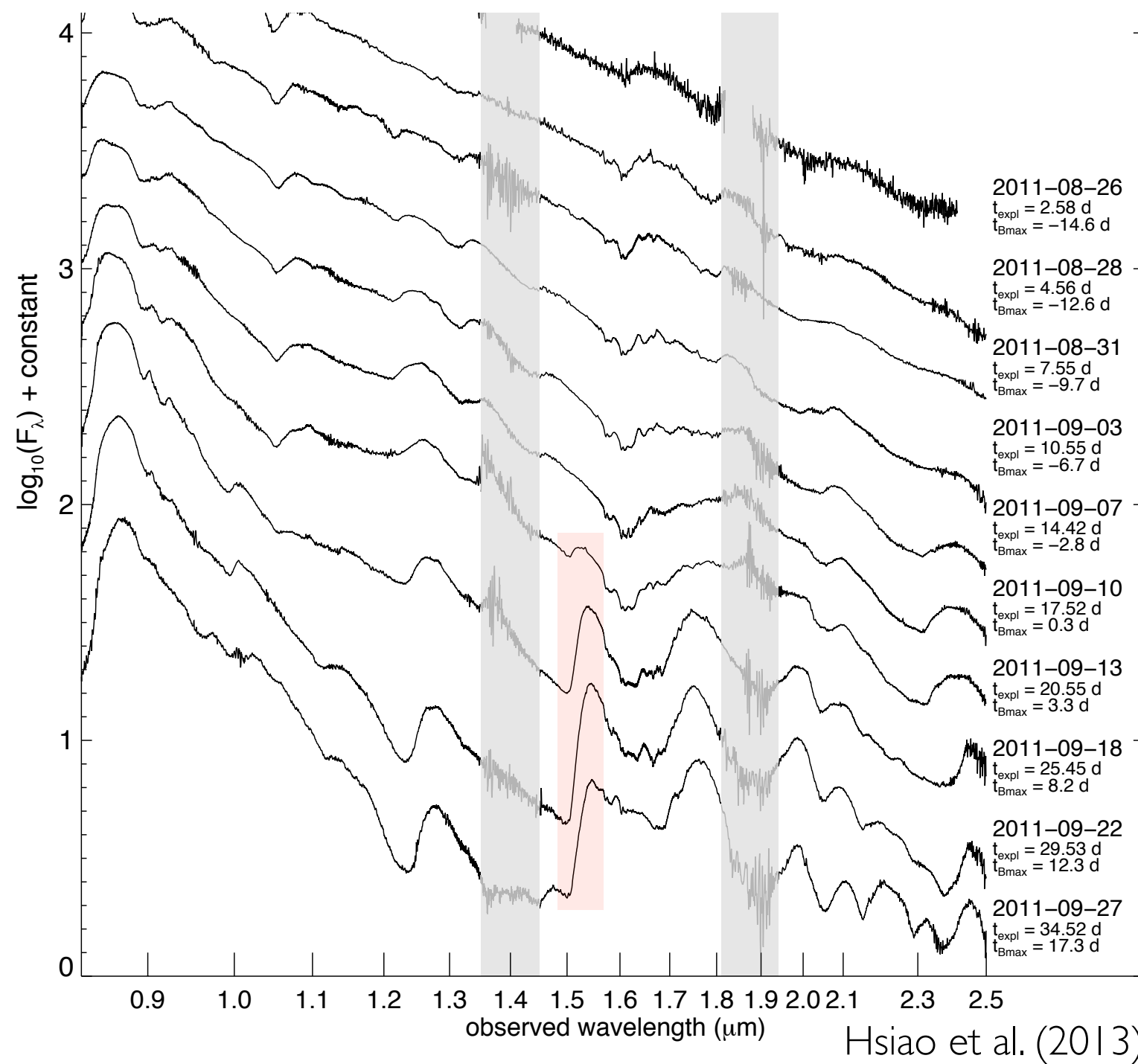


Hsiao et al. (2013)

- No correlation with light-curve decline rate
- Asymmetry may also play a role

# Radioactive nickel

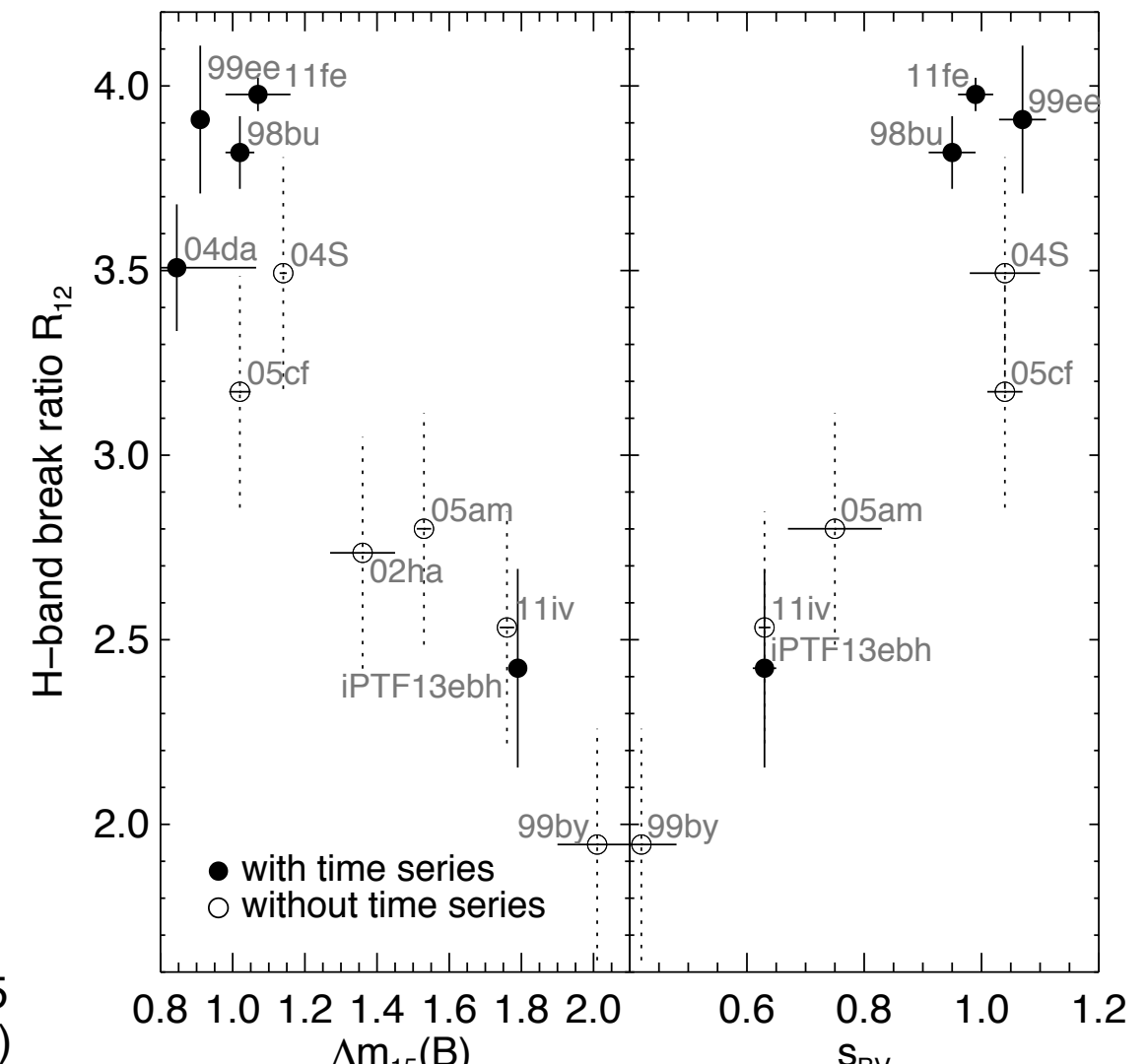
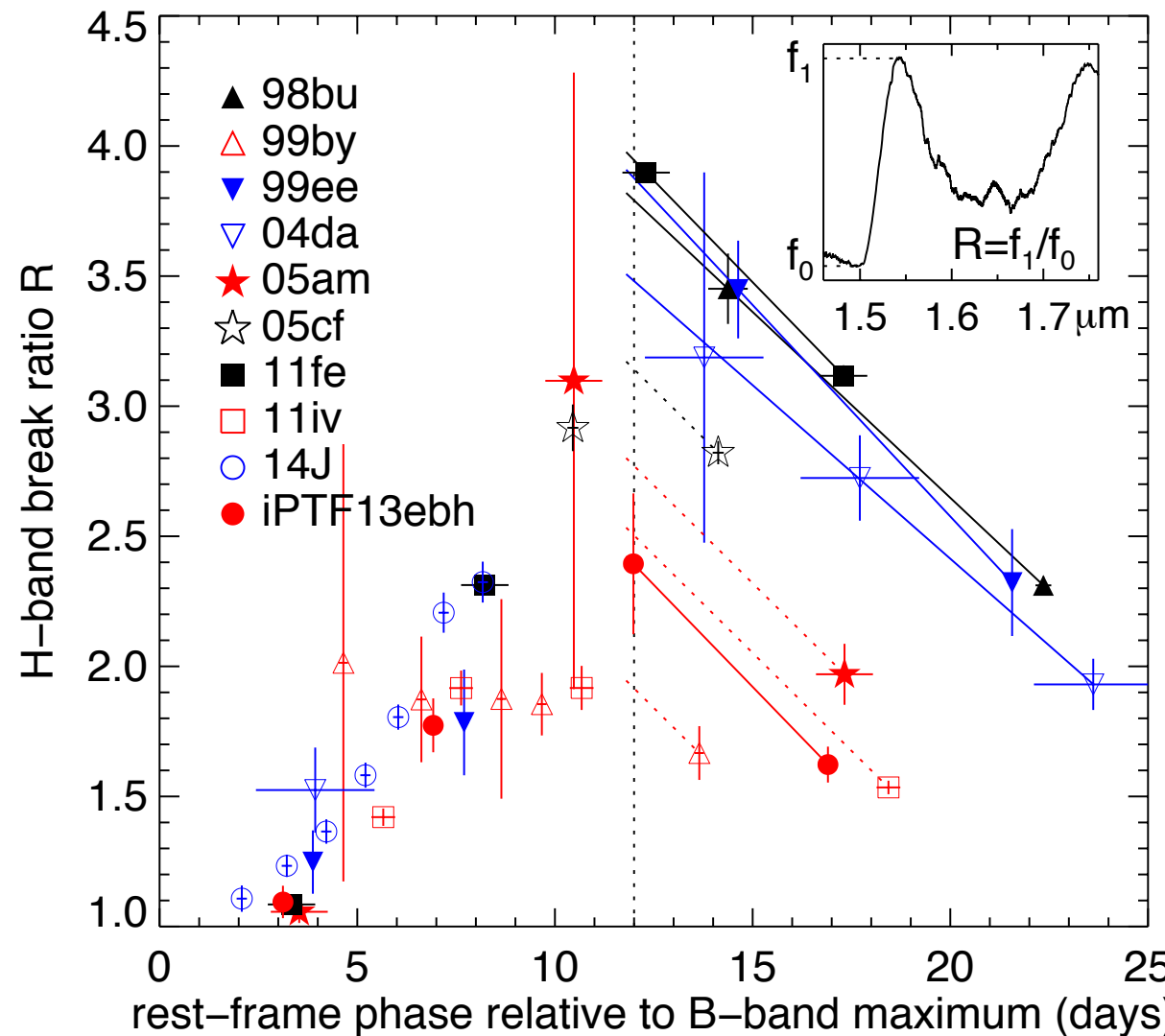
## H-band break



- H-band break:  
most prominent  
SN Ia NIR feature

# Radioactive nickel

## H-band break



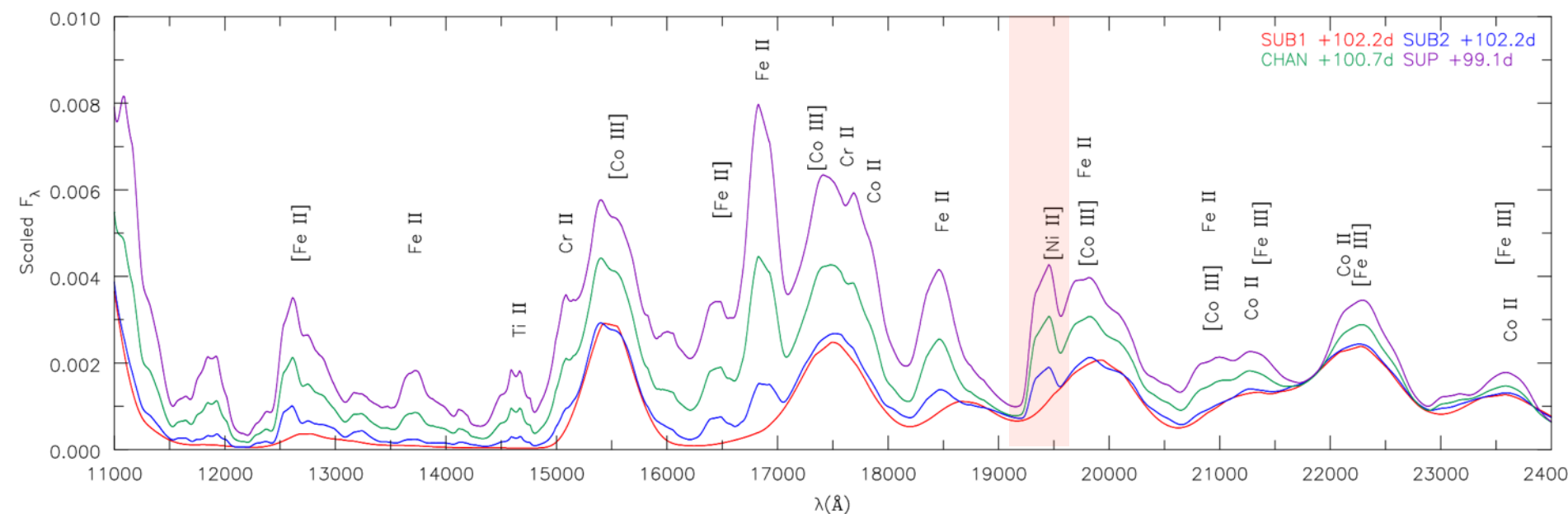
Hsiao et al. (2015)

- Strength of the break depends on the  $^{56}\text{Ni}$  mass  
Rate at which it is exposed depends on the “shielding” IME mass
- Potential to distinguish between progenitor scenarios

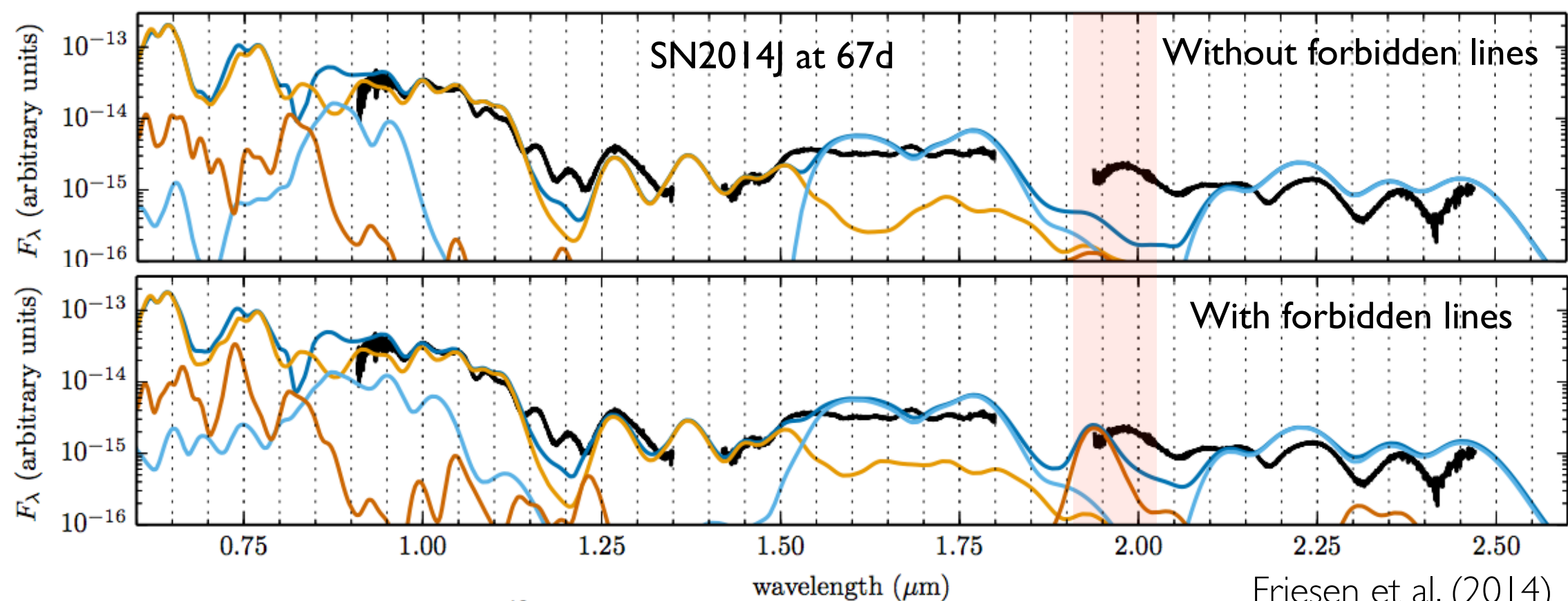
# Stable nickel

Transitional phase [Ni II] 1.939

- 1.98 micron feature: possible [Ni II]
- Nickel at late phase should be stable nickel



Wilk et al. (2018)

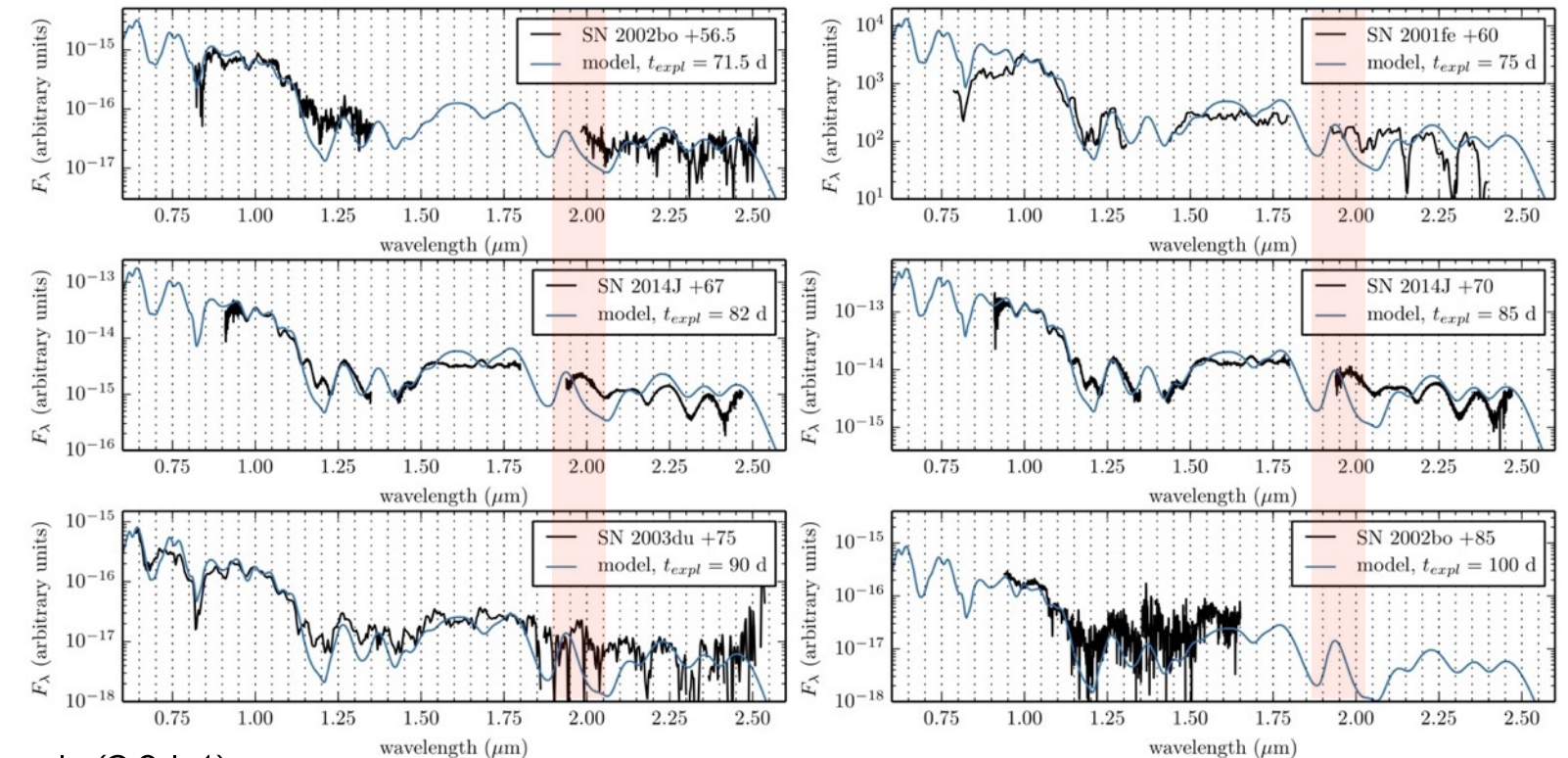
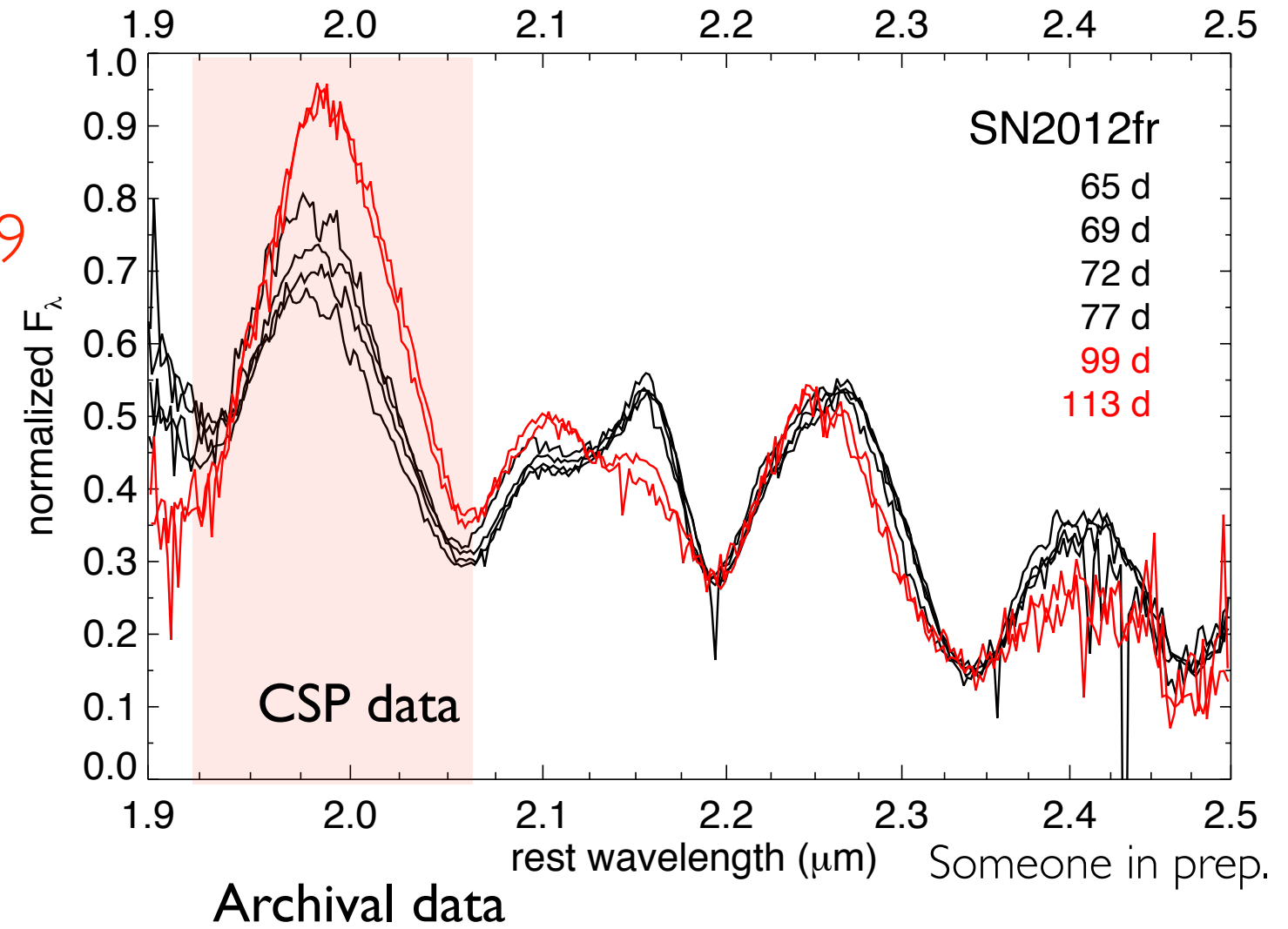


Friesen et al. (2014)

# Stable nickel

Transitional phase [Ni II] 1.939

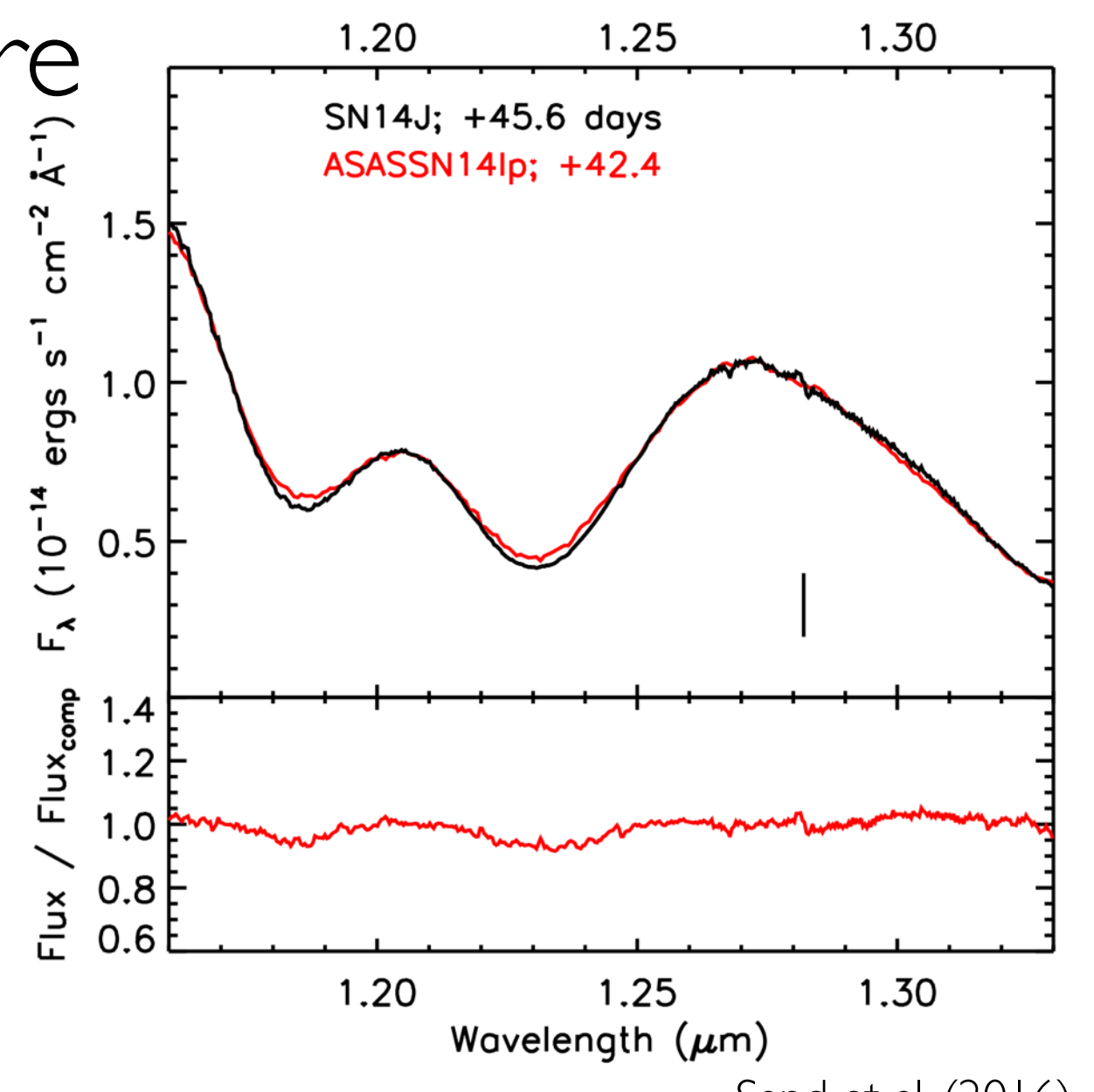
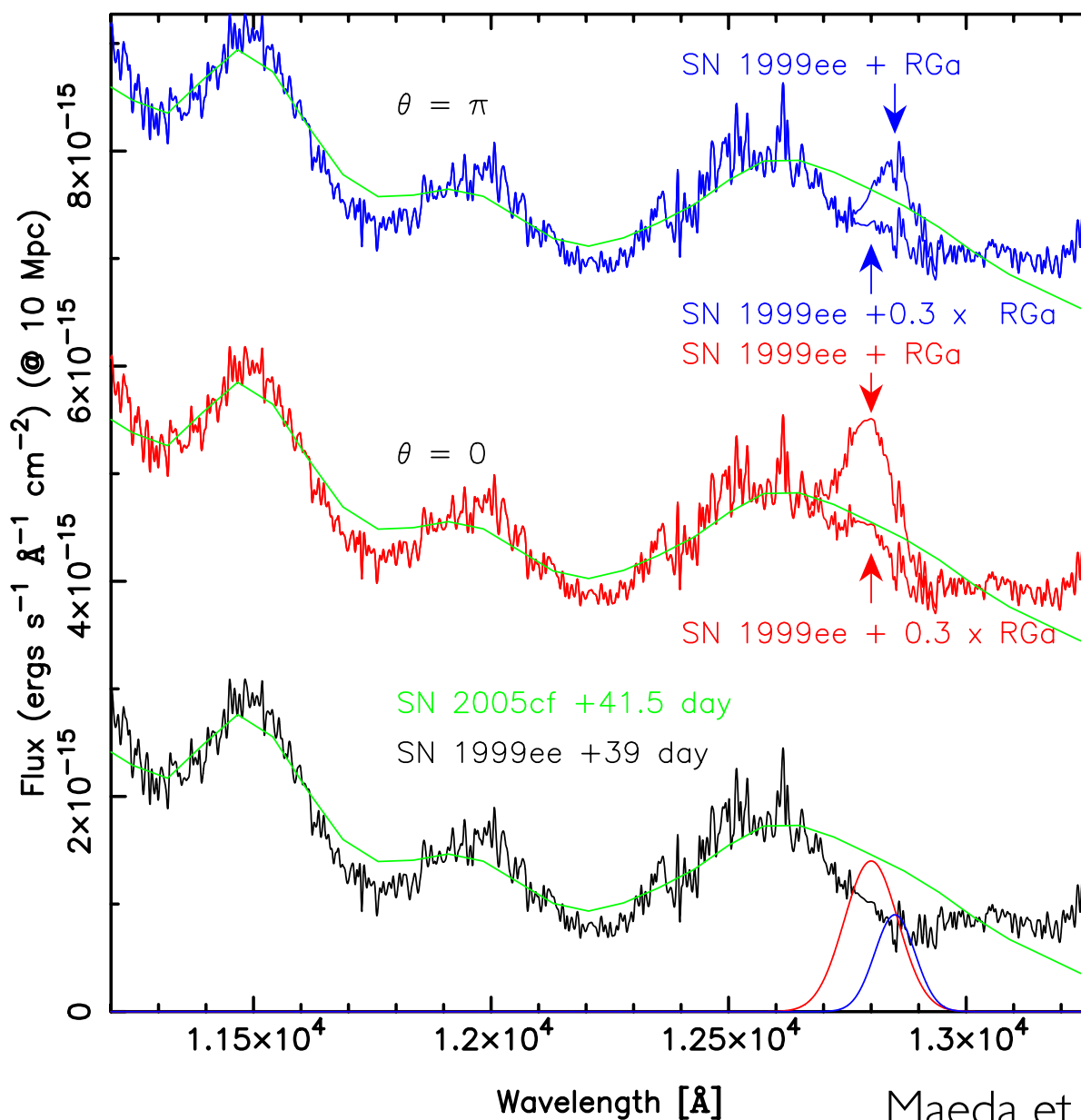
- Stable nickel can be produced only under high density condition, which in turn, is a strong indicator of a Chandrasekhar-mass explosion.
- But the strongest line in that region is always at  $\sim 1.98$  micron.



Friesen et al. (2014)

# Companion signature

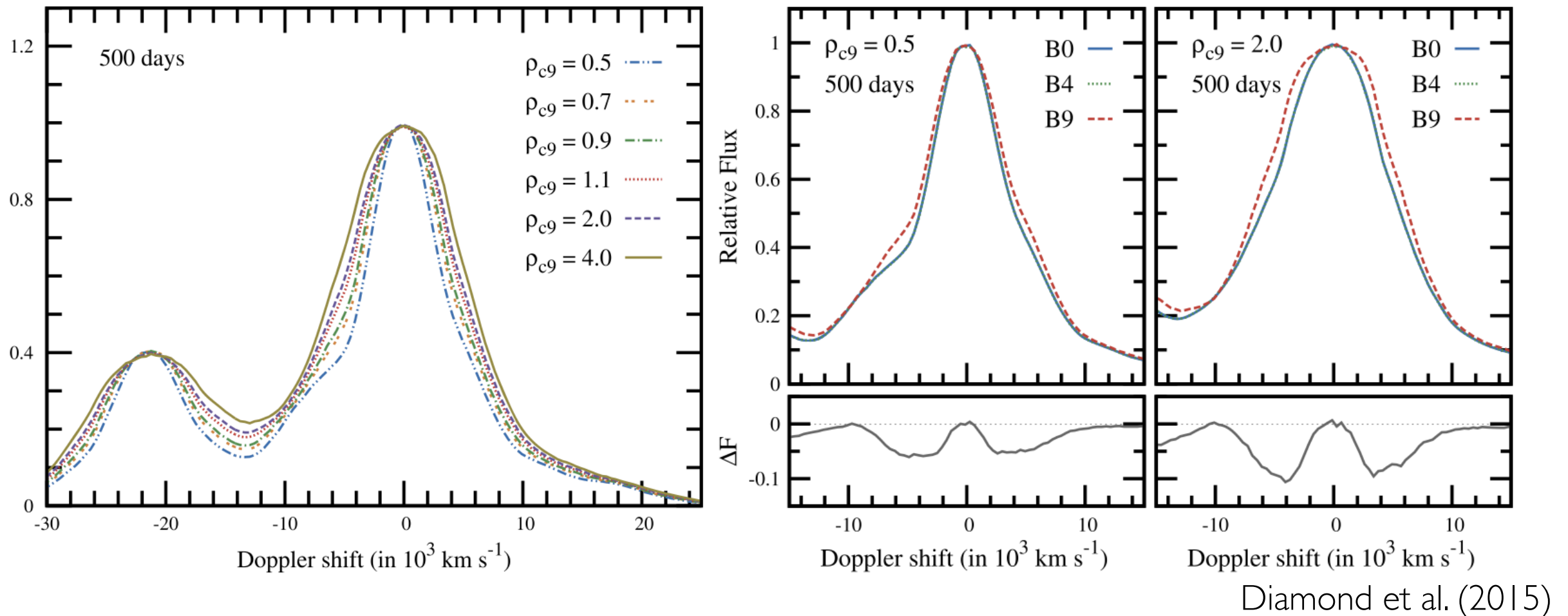
Postmax P-beta 1.282



- H stripped off non-degenerate companion, embedded at low velocity
- P-beta stronger and appear above photosphere earlier than H-alpha

# Central density and B-field

Nebular phase [Fe II] 1.6440



- Extract central density and B-field through [Fe II] line width
- Central density constraints accretion rate and progenitor system

# Probing SN Ia physics

- Unburned material  
*Premax C I 1.069, He I 1.083*  
Marion et al. (2006), Hsiao et al. (2013, 2015)
- Boundary between C/O burning  
*Premax Mg II 1.093*  
Wheeler et al. (1998), Hsiao et al. (2013)
- Radioactive nickel, ionization evolution  
*Postmax H-band break*  
Wheeler et al. (1998), Hoeflich et al. (2002), Hsiao et al. (2013)
- Stable nickel  
*Transitional phase [Ni II] 1.939*  
Friesen et al. (2014), Wilk et al. (2018)
- Companion signature  
*Postmax P-beta 1.282*  
Maeda et al. (2014), Sand et al. (2016), Botyanszki (2017)
- Central density and B-field  
*Nebular phase [Fe II] 1.644*  
Penney & Hoeflich (2014), Diamond et al. (2015), Diamond et al. (2018)